

American University in Cairo

## AUC Knowledge Fountain

---

Theses and Dissertations

Student Research

---

2-1-2013

### A proposed simplified API 579 assessment procedure for shakedown limit load determination with application to locally thinned wall pipe-branch connections

Youssef Hafiz

Follow this and additional works at: <https://fount.aucegypt.edu/etds>

---

#### Recommended Citation

##### APA Citation

Hafiz, Y. (2013). *A proposed simplified API 579 assessment procedure for shakedown limit load determination with application to locally thinned wall pipe-branch connections* [Master's Thesis, the American University in Cairo]. AUC Knowledge Fountain.

<https://fount.aucegypt.edu/etds/1277>

##### MLA Citation

Hafiz, Youssef. *A proposed simplified API 579 assessment procedure for shakedown limit load determination with application to locally thinned wall pipe-branch connections*. 2013. American University in Cairo, Master's Thesis. *AUC Knowledge Fountain*.

<https://fount.aucegypt.edu/etds/1277>

This Master's Thesis is brought to you for free and open access by the Student Research at AUC Knowledge Fountain. It has been accepted for inclusion in Theses and Dissertations by an authorized administrator of AUC Knowledge Fountain. For more information, please contact [thesisadmin@aucegypt.edu](mailto:thesisadmin@aucegypt.edu).



**The American University in Cairo**

**School of Sciences and Engineering**

***A Proposed Simplified API 579 Assessment Procedure  
for Shakedown Limit Load Determination with  
Application to Locally Thinned Wall Pipe-Branch  
Connections***

By

**Youssef Ahmed Fouad Hafiz**

A thesis submitted in partial fulfillment of the requirements for the degree of

**Master of Science in Mechanical Engineering**

Under the supervision of:

**Dr. Maher Younan**

Professor of Mechanics and Design

Associate Dean for Undergraduate Studies

School of Sciences and Engineering

The American University in Cairo

**Dr. Hany Fayek**

Assistant Professor, Mechanical Design and Solid Mechanics

Department of Mechanical Engineering

The American University in Cairo

**Fall 2012**

## ACKNOWLEDGMENTS

“Feeling gratitude and not expressing it is like wrapping a present and not giving it”. My great and first present is wrapped for Allah. Allah granted me power, patience and ability to accomplish what it was seemed to be impossible for me. Second great present is wrapped with appreciation and thanks to my supervisor Dr. Maher Younan. He was a father who taught me things that I cannot count. Even if, he was too busy in the work load upon him, he was almost available every day for me to give advice and help in research, career and life. Third great present is wrapped for my big brother before being my co-supervisor, Dr. Hany Fayek for his effort to help and support me in all master times. A special present is wrapped to thank my parents, brothers, Mohamed and Ibrahim, and my sisters, Mona and Mariam, for their support to accomplish all my achievements in my life.

“Journey best measured in friends rather than miles” during my master program, I was extremely lucky to have a journey friend like Mostafa Siam who shares me every up and down time. Also, I would like to give special thanks to all my colleagues, especially Mohammed Abd El-Aal and Ahmed Gaber. I would also to extend my thanks to mechanical department faculty and colleagues in the American University in Cairo.

I'm particularly grateful for accepting me in the fellowship by the American University in Cairo, mechanical engineering department and for the research grant and facilities offered for the master program.

## ABSTRACT

In the current research, a new assessment procedure is proposed to determine the shakedown limit load of locally thinned wall pressurized components via modifying the current API 579 level-three assessment. The new assessment procedure applies a well-established and verified simplified technique, previously developed by Abdalla et al. [1], discarding iterative full elastic-plastic cyclic loading finite element (FE) analyses. For the purpose of validation, the newly proposed assessment procedure is applied to generate the shakedown boundary of a locally thinned wall pipe-branch connection subjected to a spectrum of steady internal pressures and cyclic bending moments. The outcomes of the proposed assessment procedure are successfully verified against existing API 579 assessment procedures, numerical analyses, and experimental outcomes taken from the literature.

Interaction (Bree) diagrams illustrating elastic, shakedown, and limit load domains are constructed for the locally thinned wall pipe-branch connection problem. Additionally, a parametric study is performed through changing the both the depth and location of the local wall thinning within the pipe-branch connection. The outcomes of the parametric study show good agreement in the shakedown limit boundary results with the API 579 elastic-plastic stress analysis procedure.

## TABLE OF CONTENTS

CHAPTER 1: INTRODUCTION .....	1
1.1. Literature review .....	4
1.1.1. Local wall thinning effect .....	4
1.1.2. Limit load determination for pipe-branch connections.....	5
1.1.3. API 579 standard assessment procedures .....	8
1.1.4. Shakedown limit load determination techniques .....	9
1.1.5. Shakedown limit load determination for sound nozzle-vessel intersections .....	11
1.2. Thesis objective.....	12
1.3. Scope of work.....	13
1.4. Research outline.....	14
CHAPTER 2: SHAKEDOWN PROCEDURE AND ANALYSIS OF LOCALLY THINNED WALL COMPONENTS .....	16
2.1. Limit Load analysis .....	16
2.2. The Shakedown analysis using the Simplified Technique.....	17
2.3. The Simplified Shakedown Assessment Procedure for API 579 standard, level-three assessment.....	20
2.3.1. Overview .....	20
2.3.2. Assessment procedure.....	20
2.4. The validation case study: Locally thinned wall pipe branch connection subjected to pressure and cyclic bending moments .....	22
2.4.1. Geometry and loading of local wall thinned pipe branch connection ..	22

2.4.2.	Finite element analysis model of locally thinned wall pipe branch connection.....	25
2.5.	The existing API579 standard shakedown assessment procedures.....	29
2.5.1.	The shakedown limit assessment procedure using an elastic-plastic analysis (API 579 standard).....	29
2.5.2.	The shakedown limit assessment procedure using an approximate elastic analysis (API 579 standard) .....	31
CHAPTER 3: MODEL VERIFICATION STUDIES.....		33
3.1.	First verification study: Limit load pressure of a straight tube with external wall thinning .....	33
3.2.	Second verification study: Limit pressure of locally thinned wall pipe-branch connection .....	37
3.3.	Verification of the model of locally thinned wall pipe-branch connection using API 579 standard limit pressure assessment procedures.....	40
3.3.1.	Area replacement method .....	40
3.3.2.	Limit analysis method.....	44
CHAPTER 4: RESULTS AND DISCUSSION.....		48
4.1.	Limit load analysis .....	48
4.1.1.	Limit load analysis for sound pipe-branch connections .....	50
4.1.2.	Limit load analysis for locally thinned wall pipe-branch connections .	51
4.2.	Shakedown limit load analysis.....	57
4.2.1.	The shakedown limit boundary curves .....	60
4.2.2.	The effect of the local wall thinning depth on the shakedown limit load	64
CHAPTER 5: SHAKEDOWN RESULTS VERIFICATION USING API 579 STANDARD, LEVEL-THREE ASSESSMENT PROCEDURES .....		66

5.1.	Shakedown limit assessment (elastic stress analysis) .....	66
5.2.	Shakedown limit assessment (elastic-plastic stress analysis) .....	67
CHAPTER 6: CONCLUSION .....		71
6.1.	The limit load analysis .....	71
6.2.	The shakedown analysis.....	72
References.....		74

## LIST OF TABLES

Table 1: Geometrical parameters of the modeled pipe branch connection and its local wall thinning .....	24
Table 2: Comparison of the results of a straight locally thinned wall tube (verification study. 1).....	36
Table 3: Comparison of the results of locally thinned wall pipe-branch connection limit pressure (verification study 2) .....	39
Table 4: Area replacement method variables' selected values.....	42
Table 5: Comparison of the Simplified Technique results with API 579, Shakedown limit assessment using elastic stress analysis.....	67



## LIST OF FIGURES

Figure 1: Elastic and elastic-plastic analyses in the Simplified Technique [28] .....	19
Figure 2: Locally thinned wall pipe-branch connection geometry and boundary conditions.....	23
Figure 3: FE model of the pipe-branch connection and locations of local wall thinning highlighted (in-plane bending).....	25
Figure 4: pipe-branch connection FE model and locations of local wall thinning highlighted (out-of-plane bending).....	26
Figure 5: In-plane bending model boundary conditions .....	27
Figure 6: Out-of-plane bending model boundary conditions.....	28
Figure 7: Moment application and reference node .....	29
Figure 8: Elastic-plastic shakedown analysis loading/unloading scheme (API 579) .	30
Figure 9: Elastic shakedown analysis [2].....	32
Figure 10: Maximum strain at the middle of local wall thinning area, Hui and Li SG 690 tube experiment [3] .....	33
Figure 11: Model of SG 690 straight tube with symmetry planes and local wall thinning area.....	34
Figure 12: Typical mesh of quarter-model for SG 690 straight tube with external local wall thinning region .....	35
Figure 13: Load-Deflection diagram of Hui and Li experiment (specimen. 1) [3] ....	36
Figure 14: Twice-Elastic Slope method on load-deflection diagram of the FE model (specimen. 1).....	36

Figure 15: Quarter and half models used in the 2nd verification study; shaded regions are the local wall thinning areas.....	38
Figure 16: Limit pressure using Twice-Elastic Slope (case 1) .....	39
Figure 17: Typical pipe-branch connection areas for Area Replacement Method of API 579 [4] .....	41
Figure 19: Comparison of results of area replacement method vs. limit analysis method vs. developed FE model.....	46
Figure 20: Limit in-plane moment with the presence of 3 MPa pressure and 0.5 $d_{wt}/t$ ratio .....	49
Figure 21: Limit moment determination using Twice-Elastic Slope method in moment vs. rotational disp. Diagram.....	49
Figure 22: Comparison of the limit boundary of out-of-plane moment with Tabone and Mallette formula.....	50
Figure 23: Comparison of the limit boundary of in-plane moment with Xuan et al. numerical results .....	51
Figure 24: In-plane moment limit boundary when the local wall thinning lies on the run-pipe.....	52
Figure 25: Out-of-plane moment limit boundary when the local wall thinning lies on the run-pipe .....	52
Figure 26: Bending moment diagram a pipe-branch connection when it is subjected to bending moment on the branch.....	53

Figure 27: In-plane moment limit boundary when the local wall thinning lies on the branch.....	55
Figure 28: Out-of-plane moment limit boundary when the local wall thinning lies on the branch.....	55
Figure 29: Bree diagram of a pipe-branch connection with $0.5 d_{wt}/t$ local wall thinning and subjected to in-plane bending.....	59
Figure 30: In-plane shakedown limit boundary when the local wall thinning lies on the run-pipe .....	60
Figure 31: Out-of-plane shakedown limit boundary when local wall thinning lies on the run-pipe .....	61
Figure 32: In-plane shakedown moment limit boundary when the local wall thinning lies on the branch .....	62
Figure 33: Out-of-plane shakedown moment limit boundary when the local wall thinning lies on the branch.....	63
Figure 34: The effect of the local wall thinning depth on the in-plane and out-of-plane bending moments, when it lies on the branch.....	64
Figure 35: The effect of the local wall thinning depth on the shakedown pressure, when it lies on the branch at max tension side of in-plane and out-of-plane situations .....	65
Figure 36:Equivalent stress-equivalent plastic strain curve for reversed plasticity behavior.....	69
Figure 37: Von Mises stress-equivalent plastic strain curve for ratcheting behavior. .	70

## NOMENCLATURE

$A_r$	Required reinforcement area.
$A_1$	Available reinforcement area resulting from excess thickness in the shell.
$A_2$	Available reinforcement area resulting from excess thickness in the nozzle or run pipe.
$C_s$	Local wall thinning on the run pipe
$D$	Run pipe nominal diameter
$D_i$	Internal diameter of the run pipe
$E_1$	The joint efficiency of the weld joint; 1.0 When the opening is in solid plate or in a Category B butt joint.
$F$	Applied net-section axial force, use a negative value if the axial force produces a compressive stress at the location of the assessment point.
$L$	Run pipe length
$L_{wt}$	Local wall thinning length parallel to the pipe axis
$M_i$	Incremental moment load for elastic-plastic analysis
$M_L$	$= \frac{M}{YZ}$ ; Normalized limit moment of the structure
$M_{norm}$	Normalized moment to limit bending moment applied on a straight thin pipe
$M_{ref}$	Reference moment load for elastic analysis
$M_{SD}$	Shakedown limit moment of the structure
$M_{SL}$	Limit moment of the structure when it is applied solely
$P_L$	$= \frac{PD}{2YT}$ ; Normalized limit pressure of the structure
$P_{norm}$	Normalized pressure to the limit pressure applied on a straight thin pipe
$P_{SD}$	Steady shakedown pressure, when to apply any cyclic moment load value leads to ratcheting failure.

$P_{SL}$	Limit pressure of the structure when it is applied solely
$T$	Run pipe thickness
$Y$	Yield strength of the material
$Z$	Section modulus of tube for bending
$Z_p$	Section modulus of tube for torsion
$d$	Branch pipe nominal diameter
$d_c$	Diameter of the circular opening, or chord length at the run pipe wall mid-surface of a non-radial opening, in the plane under consideration including the effects of metal loss and future corrosion allowance.
$d_{WT}$	Local wall thinning depth
$f_{r1}$	Strength reduction factor; $f_{r1} = Y(\text{run pipe})/Y(\text{branch})$ for a set-in nozzle, $f_{r1} = 1$ for a set-on nozzle.
$f_{r2}$	Strength reduction factor; $f_{r2} = Y(\text{run pipe})/Y(\text{branch})$
$h$	Height of the elliptical head measured to the inside surface or the inside nozzle projection.
$J_r$	Load factor for external pressure
$t$	Branch pipe thickness
$t_{mm}$	Minimum measured thickness
$t_{nom}$	Nominal thickness
$w_h$	Weld leg size of the nozzle-to-vessel attachment weld on the inside surface of the vessel.
$\theta$	Local wall thinning circumferential width
$\sigma_E$	Equivalent stress field from elastic analysis
$\sigma_{ELPL_i}$	Equivalent stress field from elastic-plastic analysis
$\sigma_{r_i}$	Equivalent residual stress field calculated in each increment

## CHAPTER 1: INTRODUCTION

Fitness-For-Service (FFS) assessment is a quantitative engineering evaluation for in-service pressurized components that are degraded and may contain flaws or damage. Several damages can be assessed such as cracks, local or general wall thinning, hydrogen blisters, etc. To demonstrate the component's performance and applied stresses with the presence of the aforementioned flaws, API 579 standard is concerned with the FFS assessment that aids for a decision of run-repair-replace for such components to safely operate the plant.

API 579-1/ASME FFS-1 standard [2] is associated for analysis of degraded pressurized components. It has three levels of assessment according to the complexity of the assessment procedure. For example, limit pressure analysis of a locally thinned wall straight pipe is a level-one assessment, but for a locally thinned wall pipe-branch connection is a level-two assessment. These assessment levels are based on closed form analytical solutions. On the other hand, level-three assessment, which includes shakedown analysis, is based on finite element (FE) analysis.

Not only do pressurized components suffer from conventional applied loads, but they also suffer from several environmental effects such as erosion and corrosion. Erosion and corrosion effects can be found from the inside running fluid or outside corrosion from moisture or acidic media. All these types of attacks lead to general and localized metal loss. General metal loss is a reduction of the average thickness of the component that leads to a higher stress level, as it is inversely proportional to the thickness. The other type is localized metal loss (local wall thinning) which is more

critical as it causes stress concentration that leads to accelerated failure within the service life of the component. Therefore, design codes, in general, account for “corrosion allowance”. Corrosion allowance is an excess thickness which is added to the design thickness. Corrosion allowance may reach 12.5% of the total thickness to allow for local wall thinning to occur while maintaining the remaining thickness safe for the applied loads, but not safe for stress concentration.

In designing a new pressurized component utilizing ASME B31, the yield strength or fraction of the yield strength is used to determine the safety margin for the design. On the other hand, the fraction of yield strength is not applicable within API 579 as it deals with complex flaws, damages and degraded components. It would be too conservative to apply the fraction of yield strength as an assessment limit since flaws like cracks are already within the plastic zone and local wall thinning has severe stress concentration. Instead, elastic-plastic analysis is used to determine the “Remaining Strength Factor” (RSF). RSF is a fraction of the design load for the component based on elastic-plastic/nonlinear stress analysis such as limit load, shakedown or creep limit analysis. This factor describes the applicability of these components to continue in service with a re-rated load.

The limit load, as a failure criterion in API 579, is only applied for steady loads which are generally uncommon in pressurized components. Most of pressurized components operate under low cycle fatigue conditions which require the determination of the shakedown limit load for safe operation. Full elastic-plastic cyclic loading FE analyses are implemented by API 579 standard. Such lengthy time

consuming analyses cannot determine the RSF (RSF = limit or plastic collapse load of damaged component / limit or plastic collapse load of undamaged component) for the component directly. It just performs the analysis based on the design load and checks if a given load is safe or not according to the failure criteria. [2]



## ***1.1. Literature review***

### ***1.1.1. Local wall thinning effect***

Local wall thinning was studied as a defect within many pressurized components to evaluate its effect on the limit load. Ono et al. [3] determined the fracture behaviors of deferent types of circumferential local wall thinning of pipes, and Kim et al. [4] determined the burst pressure of locally thinned wall elbows. Mainly, geometry and location of local wall thinning were the main parameters considered to determine the limit load. Hui and Li [5] performed experimental testing to study the effect of the local wall thinning on the limit pressure of a straight pipe. Experiments were conducted on steam generator tubes with different local wall thinning flaw shapes (rectangular, arc and circumferential hoop), depths, lengths and circumferential angles at the mid span of the tube. Internal pressure was increasingly applied till burst. Load-deflection curves were plotted at the point of maximum bulging displacement, which is the radial displacement in the middle of the local wall thinning area. The Twice- Elastic-Slope method was utilized to determine limit pressures of the tubes tested. Results revealed that the local wall thinning depth is the major parameter affecting the limit pressure capacity of the tubes. The outcomes of Hui and Li [5] also showed that the longitudinal and circumferential lengths had noticeable effect up to a certain limit.

### 1.1.2. *Limit load determination for pipe-branch connections*

Plastic limit load for a sound piping branch connection was studied with applied internal pressure and/or moment loadings analytically [6], experimentally [7] [8], numerically [9] [10] [11] and including a crack [12] in order to reach closed form solutions and numerically acceptable solutions in comparison with conducted experimental outcomes. Additionally, the closed form and numerical solutions focused on the global collapse at the intersection vicinity between the run pipe and branch were most failures mainly occurred.

Schroeder [7] conducted five limit moment experiments on 40 NPS (nominal pipe size) ANSI B16.9 Grade-B carbon steel pipe branch connections subjected to in-plane and out-of-plane bending moments applied on the branch. Schroeder [7] plotted moment-rotational displacement curves for each test to apply four different limit load techniques namely: the tangent intersection method, the plastic modulus method, the three-delta method, and the plastic load method. Outcomes of the five employed limit load techniques illustrated that the experimental limit moments were significantly lower than the theoretical limit load of a straight pipe having the same NPS and material. Schroeder [7] concluded that the tangent intersection method had the most consistent results.

Xuan et al. [6] developed a closed form solution for a pipe-branch connection subjected to out-of-plane bending moment by employing two material models namely: an elastic-perfectly-plastic and a linear strain hardening. “Global collapse of

the intersection due to plastic hinges forming along intersection line” was selected as the mode of failure as it is the most commonly employed mode of failure in the petrochemical industry depending on experimental data of Schroeder [7]. Xuan et al. [11] closed form solution was verified using Schroeder [7] experimental outcomes. Additionally, Xuan et al. [11] developed FE models using continuum 3D 20-noded elements and the same material employed within their closed form solution. The Twice-Elastic-Slope method was also used to determine the limit load from the generated load-displacement curves. Both the closed form solution and the FE results were in good agreement with the experimental outcomes.

Malette and Tabone [13] developed an FE model for a standard pipe-branch connection geometry. Internal pressure, out-of-plane bending moment applied on the branch and a combination of both loadings were applied to determine the limit load for the three loading cases individually. The limit load was determined through extrapolation of the inverse of the displacement readings. For the case of combined internal pressure and bending moment, the limit moment decreased by 35% compared to the case where the bending moment was only applied. Malette and Tabone [13] described the interaction expression of the limit loads as follows:

If the independent limit loads were considered, the interaction is expressed as

$$P_L \leq 1 \quad \text{and} \quad M_L \leq 1 \quad (1)$$

If the combined effect comes from direct superposition, the interaction is expressed as

$$P_L + M_L \leq 1 \quad (2)$$

Finally, the numerical results of the combined loads were closely approximated as

$$P_L^2 + M_L^2 \leq 1 \quad (3)$$

$$\text{Where } M_L = \frac{M}{M_{SL}} \text{ and } P_L = \frac{P}{P_{SL}} \quad (4)$$

In particular, a branched pipe connection that includes local wall thinning has been numerically analyzed by Lee et al. [14] [15]. The branched pipe connection was subjected to a spectrum of steady internal pressures and in-plane and out-of-plane bending moments respectively employing an elastic-perfectly-plastic material model. Local wall thinning depth and longitudinal and circumferential lengths were the main parameters studied by Lee et al. [14] [15]. The FE outcomes complied well with two closed form solutions of two analytical equations available within the literature. The first closed form solution determined the limit pressure of a circumferential internal part-through cracks of a straight pipe [16], while the second closed form solution determined the limit pressure of a sound pipe-branch connection [9]. Lee et al. [14] [15] found that if the local wall thinning lies on the run pipe, failure may occur at the intersection between run and branch pipes; hence, the first closed form solution can be applied. For the same local wall thinning location, failure may occur in the thinned region; hence, the second closed form solution can be applied. On the other hand, if the local wall thinning lies on the branch next to the intersection between run and branch pipes, the failure occurs at the thinned region at the intersection. Therefore, the first solution can be applied with some modifications to describe the geometry of the local wall thinning. Lee et al. [14] [15] concluded that the limit pressure is the critical load of the two analyzed cases.

### 1.1.3. API 579 standard assessment procedures

API 579 assessment procedures is applied to locally thinned wall pipe-branch connections to determine the limit load and shakedown limit load (shakedown determination analysis is termed “ratcheting analysis” in API 579 standard) using part-five, level-two assessment and Annex B1 level-three assessment respectively [2]. For the limit pressure assessment procedure, there are two methods employed in API 579. “Limit analysis method” is for unreinforced nozzles and pipe-branch connections which are fabricated from ferrous material with yield to ultimate tensile strengths ratio ( $YS/UTS$ )  $< 0.8$ . The other method is the “area replacement method” employed for unreinforced or reinforced pipe branch connections. This method is known to produce conservative results for small nozzles. For both assessment procedures, any mechanical applied load other than pressure is not included in the evaluation of the acceptability of the pipe-branch connection [2].

For the shakedown limit load determination, there are two types of analyses. The first is an approximated elastic analysis, and the second is a full elastic-plastic cyclic loading numerical analysis. The previously mentioned numerical analysis methods are categorized as level-three assessment procedure in API 579.

The elastic analysis is similar to the twice-elastic limit method which is employed in B31 design codes [17]. More specifically, the elastic analysis considers its yield strength double the yield strength of the pressurized component material. As the elastic limit is reached, its corresponding load is considered as the shakedown

limit load of the component. The elastic analysis method is very conservative when applied to geometrically complex components subjected to multi-axial loading conditions. Contrarily, the elastic analysis method is the simplest analysis method that could be applied for determination of shakedown limit loads.

Second, the elastic-plastic analysis is a typical cyclic load applied statically on the structure to plot the major plastic deformation, thus the shakedown limit load can be determined. This later technique is only a check for safe or fail of a given load; therefore, if it is used for shakedown limit determination, it should be iteratively repeated till reach the limit. On the other hand, it can show the failure mode of the structure with the given load whether it is ratcheting or reversed plasticity in the load-deflection curve [2].

#### 1.1.4. Shakedown limit load determination techniques

Melan [18] was the first to introduce the lower bound shakedown theory in the late thirties of the previous century, which is stated as follows: *“For a given cyclic load set (P), if any distribution of self-equilibrating residual stresses can be found (assuming perfect plasticity) which when taken together with elastically calculated stresses constitute a system of stresses within the yield limit, then (P) is a lower bound shakedown load set and the structure will shakedown.”* The theory shows that the shakedown limit load is reached when the residual stresses in a component equals to the yield limit. Later, in the mid-sixties, several iterative elastic techniques implementing FE analyses have been developed to determine the shakedown limit, such as the GLOSS R-Node [19], the thermo-parameter method [20] and the elastic

compensation method (ECM) [21]. The ECM [21] is the most common utilized technique. It is based on a numerical elastic analysis for the nominal design load, followed by a series of iterations modifying the elastic moduli as shown in equation (5). As the shakedown stress field, resulted from every iteration, is the summation of residual and elastic stresses, the residual stresses can be obtained, as shown in equation (6); hence, if a residual stress field, for a specific trial, is equal to or greater than the yield strength of the material, the minimum corresponding load for this trial can be considered as the shakedown limit load.

$$E_i = E_{i-1} \frac{\sigma_n}{\sigma_{i-1}} \quad (5)$$

$$\sigma_{r_i} = \sigma_{s_i} - \sigma_e \quad (6)$$

Ponter and Carter [22] developed a nonlinear programming method called Linear Matching Method (LMM) to solve nonlinear problems such as shakedown limit by enforcing the convergence of the nonlinear solution to a limited number of linear problems. Every linear problem is an ECM problem. In other words, LMM is a generalization of ECM to solve any nonlinear problem. It was applied to shakedown and creep as well.

A Simplified Technique was developed by Abdalla et al. [1] [23] [24] to determine shakedown limit loads. It is based on performing only two FE analyses namely: an elastic analysis and an elastic-plastic analysis. Residual stresses are determined through subtracting the outcomes of the two analyses. The shakedown

limit can be defined when the residual stresses reach a yield limit of tension or compression as stated in the Melan theorem. Abdalla et al. [1] [23] [24] verified this technique by comparing the generated results from the technique with several experimental data and bench mark problems, such as 2-bar and Bree cylinder models. Results showed good agreement with an acceptable accuracy; hence, the Simplified Technique was applied on 90-degree pipe bends and cylindrical nozzle-vessel intersections. Both applications were subjected to steady internal pressure and alternating bending moments to obtain their shakedown limit boundary without long time consuming numerical iterations. Therefore, the Simplified Technique was chosen to be used in the current research. It will be illustrated in detail in section 2.2.

#### *1.1.5. Shakedown limit load determination for sound nozzle-vessel intersections*

Nadarajah et al. [25] determined the upper and lower bound shakedown limit load for sound cylindrical nozzle-vessel intersection, subjected to internal pressure and in-plane bending moment using the ECM. With these shakedown analyses, Nadarajah et al. [25] found that the nozzle can be loaded three times more than the initial yield load, with some plastic deformation, and without gross deformation of the entire structure. Results showed to be closer to the upper shakedown limit for Macfarlane and Findlay [26] than the lower shakedown limit for Robinson [27] with a discrepancy of 50%. Nadarajah et al. [25] attributed this discrepancy as the FE mesh in the model was not properly refined, but the average of the two results would be a good estimate of the limit boundary.



## ***1.2. Thesis objective***

The objective of this thesis is to propose the Simplified Technique developed by Abdalla et al. [1] [23] as a new assessment procedure for API 579 standard. The main motive in developing this procedure is to replace the current elastic-plastic analysis in API 579 level-three assessment to help for run-repair-replace decision. The second objective is to validate the simplified shakedown assessment procedure to be implemented for locally thinned wall pressurized components. Therefore, the shakedown limit load is determined through a direct non-cyclic method (the Simplified Technique) regardless of the existing API 579 time consuming full elastic-plastic numerical analyses.

### ***1.3. Scope of work***

The scope of the current research is directed towards validating the proposed simplified assessment procedure to be implemented for locally thinned wall pressurized components. The validation is achieved through applying the proposed assessment procedure to determine the shakedown limit for a pipe-branch connection including local wall thinning, and verifying the outcomes of the validation with the existing shakedown assessment procedures in API 579.

The pipe-branch connection of the validation case study was selected based on the available results within the literature. The pipe-branch connection is subjected to a spectrum of steady internal pressures and cyclic in-plane and out-of-plane bending moments respectively. Local wall thinning locations are selected to be on the run pipe opposite to the branch, and on the branch next to the intersection line at the maximum tension side of the bending moment on the branch. A Parametric study was conducted to examine the effect of local wall thinning depth and location, on both limit loads and shakedown limit loads, covering the range of 0 - 0.7 of the local wall thinning depth to total thickness ratio.

#### ***1.4. Research outline***

First, the simplified shakedown assessment procedure is proposed for API 579 based on a reliable study and analysis of the Simplified Technique; then the aforementioned case study is selected as a validation for the new assessment procedure. A model of a closed ended straight pipe with an external local wall thinning is developed, to verify the modeling methodology of the local wall thinning. Parameters are selected to be the same as the experimental data of Hui and Li [5] and Twice-Elastic Slope method is used to obtain the limit pressure to be compared with the experimental data.

An FE model is built for the selected verification case study of locally thinned wall pipe-branch connection. The model is verified against numerical results and two different existing procedures in API 579. The model is built, as will be illustrated in section 3.2, to have the same parameters of Lee et al. [14]. Internal pressure is applied to get also the limit pressure using Twice-Elastic Slope method. Finally, results are compared to verify the locally thinned wall pipe-branch connection FE model and make it ready to outcome reliable results.

Second and third model verifications are to compare the limit pressure results of the verified model with two API 579 limit pressure existing assessment procedures. Area replacement method and limit analysis assessment procedures are applied to the same geometry and loading of the validation case study. Also, results are compared to show the effect of the local wall thinning depth on the limit pressure.

Shakedown limit bending moment analysis is conducted on the previous model of locally thinned wall pipe-branch connection, with the existence of steady

internal pressure, using the new shakedown assessment procedure. Bree diagrams are plotted to compare these results with the existing elastic and elastic-plastic analyses in API 579 level-three assessment. This comparison proved that the proposed simplified assessment procedure has a value added to API 579 standard that merges between an acceptable accuracy, close to elastic-plastic analysis, and simplicity, close to elastic analysis.

## **CHAPTER 2: SHAKEDOWN PROCEDURE AND ANALYSIS OF LOCALLY THINNED WALL COMPONENTS**

This chapter has an illustration of the main techniques used throughout this research. First, it demonstrates the limit load determination using the Twice-Elastic Slope technique, then the shakedown analysis using the Simplified Technique as developed by Abdalla et al. [1] [23]. This is followed by the new assessment procedure determining the shakedown limit based on the Simplified Technique. The assessment procedure is presented with the same format of API 579 standard to make it familiar in usage. Then the validation case study and its FE model are demonstrated to apply limit load and shakedown limit load analyses. Finally, the two existing assessment procedures in API 579 evaluating the shakedown limit load are demonstrated. These two assessment procedures will be used later in chapter 5 to verify the results of the new assessment procedure when it is applied to the validation case study.

### ***2.1. Limit Load analysis***

Limit load of a component is the value of a specific load condition that when applied, the component experiences a drop of its load carrying capacity and a major change of its overall dimensions.

To perform limit load analysis on a component, an elastic-plastic Finite Element (FE) analysis is performed to plot load-displacement diagram. The displacement should be read from the point of maximum displacement at the same direction of applied load. For example, in a straight pipe when it is subjected to internal pressure,

the point of maximum radial displacement is read and plotted against the pressure load.

There are several techniques [19][20][21][22][23] to determine the exact limit load from the load-deflection diagram, like three-delta method, tangent intersection method and Twice-Elastic Slope method and many others. Twice-Elastic Slope method is the most common method in pressure contained problems, like straight pipes and pipe-branch connections, as shown in the literature review in chapter 1. The limit load in this method is determined from the intersection of the limit boundary and a line that has a double-slope of the elastic line.

## 2.2. *The Shakedown analysis using the Simplified Technique*

Melan's lower bound shakedown theory [18] states *"For a given cyclic load set (P), if any distribution of self-equilibrating residual stresses can be found (assuming perfect plasticity) which when taken together with elastically calculated stresses constitute a system of stresses within the yield limit, then (P) is a lower bound shakedown load set and the structure will shakedown."* From Melan's theory, the condition of shakedown limit load can be determined as follows; it is the load increment when it is reached, the residual stress level or the summation of the elastic and residual stresses reach the yield strength of the material, as shown in equations (7) and (8).

$$\sigma_{el} + \sigma_r = \sigma_y \quad \text{Stress level when the load is applied} \quad (7)$$

$$\sigma_r = \sigma_y \quad \text{Stress level after unloading} \quad (8)$$

The Simplified technique was developed by Abdalla et al. [1] to numerically determine the shakedown limit load without several iterations and directly applies Melan's lower bound shakedown theory. It is based on the assumptions of small displacement formulation and it neglects the strain hardening effect of the material (elastic-perfectly-plastic material model).

The Simplified Technique is applied to a component that is subjected to a steady load (P) and a cyclic load (M). It has two analyses; first analysis is an elastic analysis ( $\sigma_E$ ). The component is subjected to the cyclic load ( $M_{ref}$ ) only in a monotonic manner in one step, as shown Fig. 1(a). The second analysis is an elastic-plastic analysis ( $\sigma_{ELPL}$ ). The component is subjected to the steady load (P) in an analysis step. Then, the cyclic load ( $M_i$ ) is subjected incrementally and in a monotonic manner in a following analysis step.

For every load increment ( $M_i$ ), the elastic stress field ( $\sigma_E$ ) is multiplied by the ratio ( $\frac{M_i}{M_{ref}}$ ) to scale it to this load increment. By subtraction the scaled elastic stress field ( $\sigma_E \frac{M_i}{M_{ref}}$ ) from every increment of the elastic-plastic analysis, the residual stresses ( $\sigma_{r_i}$ ) is determined for every load increment, as in equation (9).

$$\sigma_{r_i} = \sigma_{ELPL_i} - \sigma_E \frac{M_i}{M_{ref}} \quad (10)$$

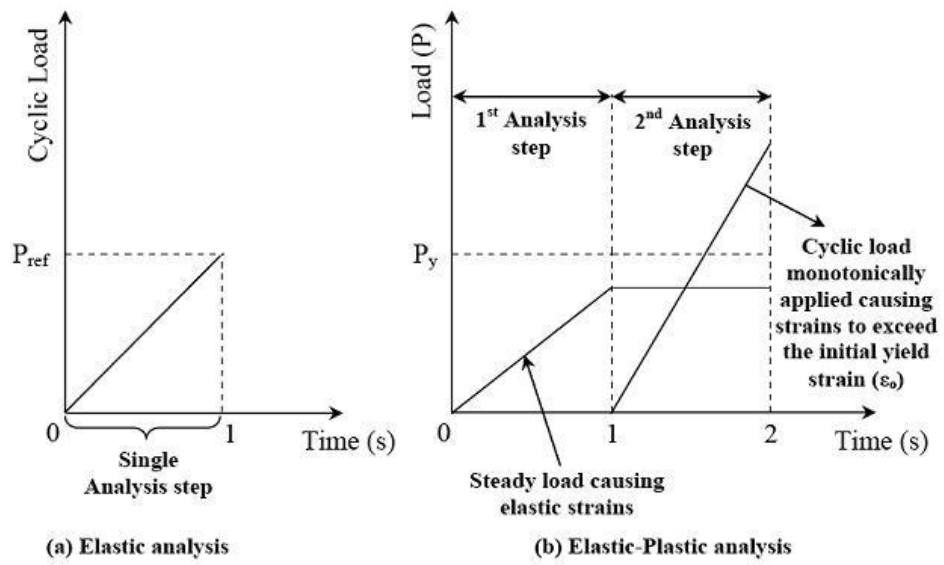


Figure 1: Elastic and elastic-plastic analyses in the Simplified Technique [28]



## 2.3. *The Simplified Shakedown Assessment Procedure for API 579 standard, level-three assessment*

### 2.3.1. *Overview*

To evaluate against ratcheting and reversed plasticity failures using elastic-plastic analysis, the shakedown limit load should be obtained. The Simplified Technique is utilized for a component that has combined steady and cyclic loads. The Simplified Technique consists of two numerical analyses. The elastic-plastic analysis ( $\sigma_{ELPL}$ ) has the alternating load ( $L_i$ ) applied in a monotonic incremental manner. The elastic analysis ( $\sigma_E$ ) has the applied alternating load in a monotonic manner also, and scaled to the same load magnitude of the previous elastic-plastic analysis ( $\frac{M_i}{M_{ref}}$ ). By subtraction the two analyses then comparing the resultant residual stresses with the yield strength incrementally, the shakedown limit load can be obtained. This analysis is based on the assumptions of elastic-perfectly-plastic material model and small displacement formulation using von Mises failure criterion. General and local wall thinning should be included in the model, by defining a thinner region in the shell with the same bottom or top surface of the neighbor shells in the FE software.

### 2.3.2. *Assessment procedure*

STEP 1 – Develop a numerical model for the component with all geometrical, flaws parameters and boundary conditions.

STEP 2 – Define the design steady and alternating loads magnitudes and cases for the component.

STEP 3 – Perform an elastic analysis for only the alternating load with any magnitude ( $L_{ref}$ ) applied monotonically to get the von Mises elastic stress field  $\sigma_E$ .

STEP 4 – Using elastic-perfectly-plastic material model, perform an elastic-plastic analysis in two steps. First step is to apply the steady load at one increment. The second step is to apply the alternating load monotonically also and incrementally but with a high value ( $L_i$ ) to ensure that the input load is higher than the expected shakedown limit load magnitude. The number of increments should be sufficient to ensure that the load increment is lower than the maximum error required. The output of this analysis is the elastic-plastic von Mises stress field for every increment  $\sigma_{ELPL_i}$ .

STEP 5 – Get the von Mises residual stresses for every increment  $\sigma_{r_i}$  from the following equation.

$$\sigma_{r_i} = \sigma_{ELPL_i} - \sigma_E \frac{L_i}{L_{ref}} \quad (11)$$

STEP 6 – the shakedown limit load  $L_i = L_{SD}$  is the load increment that corresponds to the minimum  $\sigma_{r_i}$  that equals to yield strength in tension or compression.

-If the shakedown limit load  $L_{SD}$  is higher than the design load, the component can run with the same load magnitude.

-If the shakedown limit load  $L_{SD}$  is lower than the design load, the component should be re-rated to the shakedown limit load.

## **2.4. The validation case study: Locally thinned wall pipe branch connection subjected to pressure and cyclic bending moments**

### **2.4.1. Geometry and loading of local wall thinned pipe branch connection**

As the FE model of the pipe-branch connection should be verified against limit load results of Lee et al. [14], the geometrical parameters, loading and boundary conditions of the concerned pipe-branch connection were chosen to be the same as of the Lee et al. [14] FE model. As shown in Fig. 2, the pipe-branch connection, considered in this study, is closed-ended simply-supported from both ends. It has a long run-pipe to neglect the effect of the end conditions at both ends. It does not have a reinforcement pad at the intersection, but it has only a weld fillet equals to the minimum thickness of the branch to avoid stress concentration. The run-pipe and the branch are considered to have the same material and diameter to thickness ratio ( $D/T = d/t$ ) for the sake of minimizing the number of variables to focus on local wall thinning loading variables, as the limit load is directly related to the material and diameter to thickness ratio.

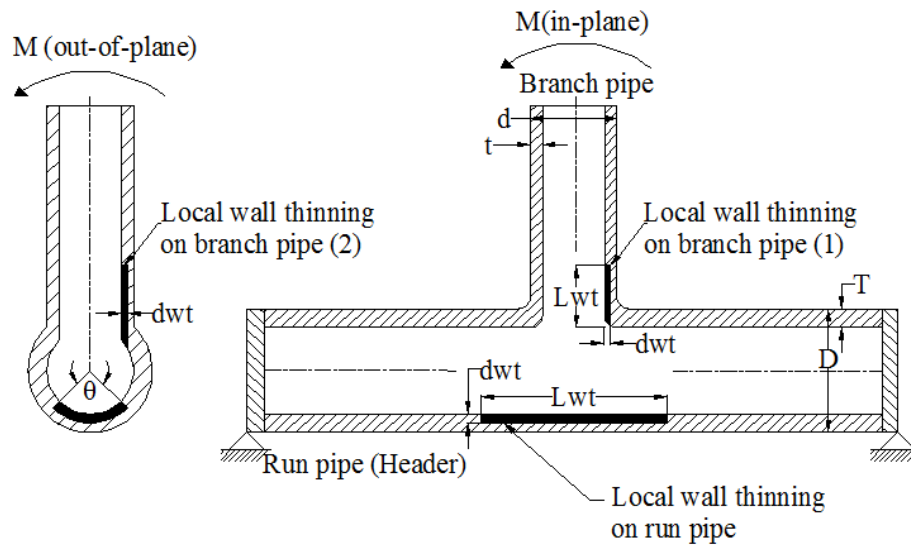


**Figure 2: Locally thinned wall pipe-branch connection geometry and boundary conditions**

For the loads applied on the pipe-branch connection, an internal pressure was applied with a shell edge load to simulate the closed ended run and branch pipes. Moments are applied on the branch in in-plane and out-of-plane directions with the center line of the run pipe.

Table (1) shows the values of the geometrical and local wall thinning parameters used in the analyses. These parameters were fixed for all in-plane and out-of-plane models except local wall thinning depth ( $d_{wt}$ ), loads (pressure and moment) and local wall thinning location are the main variables in this analysis. Local wall thinning has always the same area –same length and width also- in all cases as it has a limited effect on the limit load according to the analyses conducted by Lee et al. [14] [15].

**Table 1: Geometrical parameters of the modeled pipe branch connection and its local wall thinning**

D	T	d	T	L <sub>wt</sub>	Θ
80	4	48	2.4	160	90°

Parameters in the table were selected based on the ratios selected by Lee et al. [14] as the following:

$$R/T=10$$

$$\theta/\pi=0.5$$

$$L_{wt}/R=4$$

For the local wall thinning depth to total thickness ratio ( $d_{wt}/t$  or  $d_{wt}/T$ ), the main variable of this study, according also to Lee et al. [14] was selected to be 0, 0.5 and 0.7. As a result, these ratios have a great contribution in normalization of the results to be used by any material and geometry of pipe-branch connection or nozzle-cylindrical vessel intersection or any local wall thinning parameters. Results were normalized to a straight run-pipe subjected to a pressure and bending moment as in the equations.

$$M_{norm}(in\ plane\ bending) = \frac{M}{Y Z} \quad when \quad Z = \frac{\pi}{32} \left( \frac{D^4 - D_i^4}{D} \right) \quad (12)$$

$$M_{norm}(out\ of\ plane\ bending) = \frac{M}{Y Z_p} \quad when \quad Z_p = \frac{\pi}{16} \left( \frac{D^4 - D_i^4}{D} \right) \quad (13)$$

$$P_{norm} = \frac{PD}{2YT} \quad (14)$$

#### 2.4.2. Finite element analysis model of locally thinned wall pipe branch connection

Four FE models were developed for the pipe-branch connection considered in this study. For every in-plane and out-of-plane bending models, Figs. 3 and 4, there is a model for a local wall thinning lies on the run-pipe and another model for a local wall thinning lies on the branch at the maximum tension side of the bending moment. Due to the symmetry in geometry and loading, half models were developed using an eight-node, doubly curved and reduced integration thick shell element (S8R) with five integration points through the thickness in ABAQUS CAE/STANDARD software.

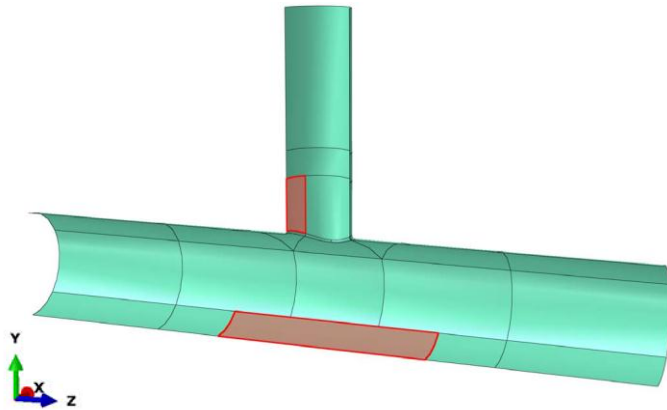


**Figure 3: FE model of the pipe-branch connection and locations of local wall thinning highlighted (in-plane bending)**

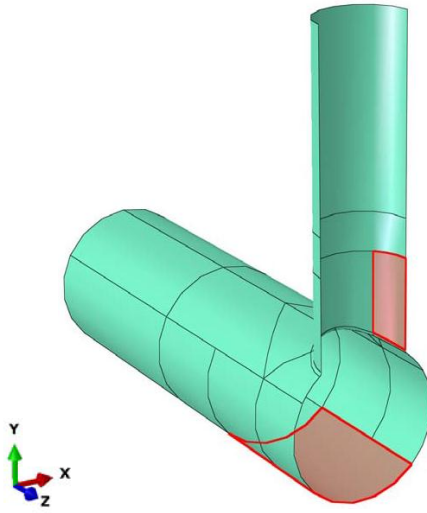


**Figure 4: pipe-branch connection FE model and locations of local wall thinning highlighted (out-of-plane bending)**

Local wall thinning region was modeled from the same shell element but with a thinner thickness and it has the same bottom surface of the sound neighboring regions. Mesh convergence study was made to achieve the optimized mesh density and scheme for the component. The material model was considered to be elastic-perfectly-plastic for limit load and shakedown limit load analyses. Except for the verification with limit load assessment procedures of API 579 standard, area replacement method and limit analysis have a limitation to have a ferrous metal with strain hardening material model required by API 579 standard, as will be illustrated in section 3.3.

According to the boundary conditions used in the models, there is a double symmetry of the geometry and loadings (pressure and moments), as shown in Figs. 5 and 6. Symmetry was taken about Y-Z plane, as shown in Fig. 5, for in-plane bending

situation. Also, symmetry was taken about X-Y plane, as shown in Fig. 6, for out-of-plane bending situation. Y-Z plane of symmetry is described in FE software by a fixation of the linear displacement in X-direction and rotation about Y and Z-directions and X-Y plane of symmetry is described by a fixation of the linear displacement in Z-direction and rotation about X and Y-directions

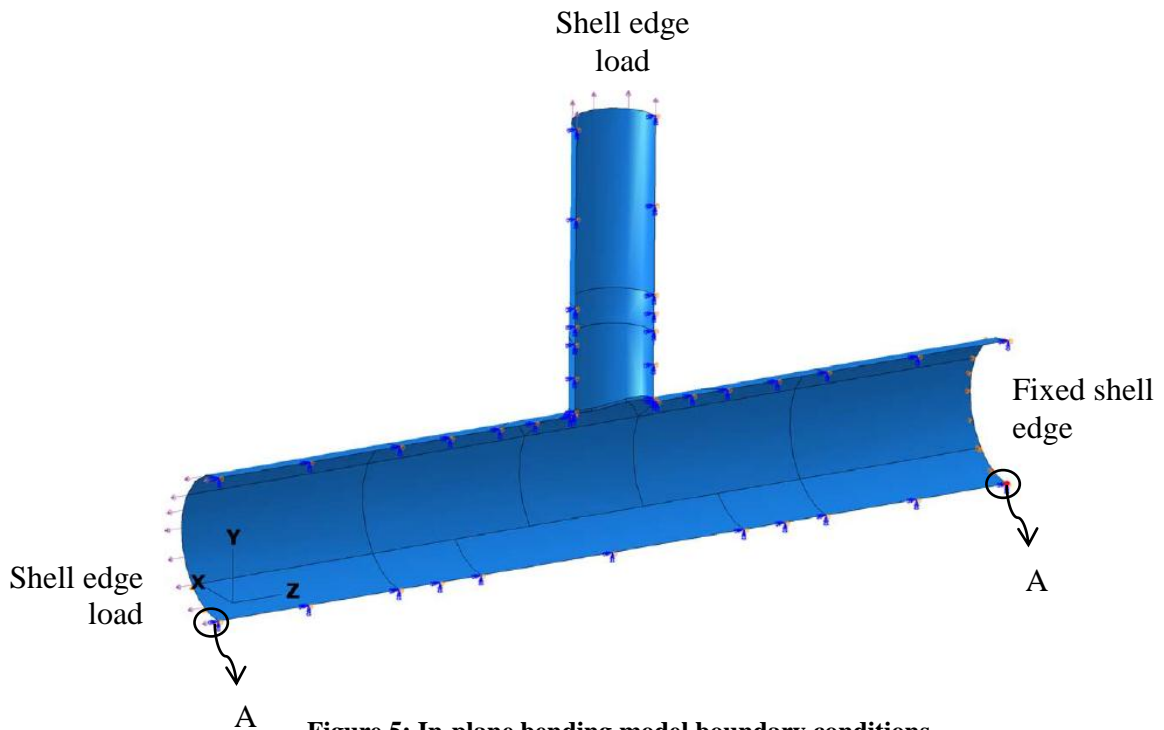
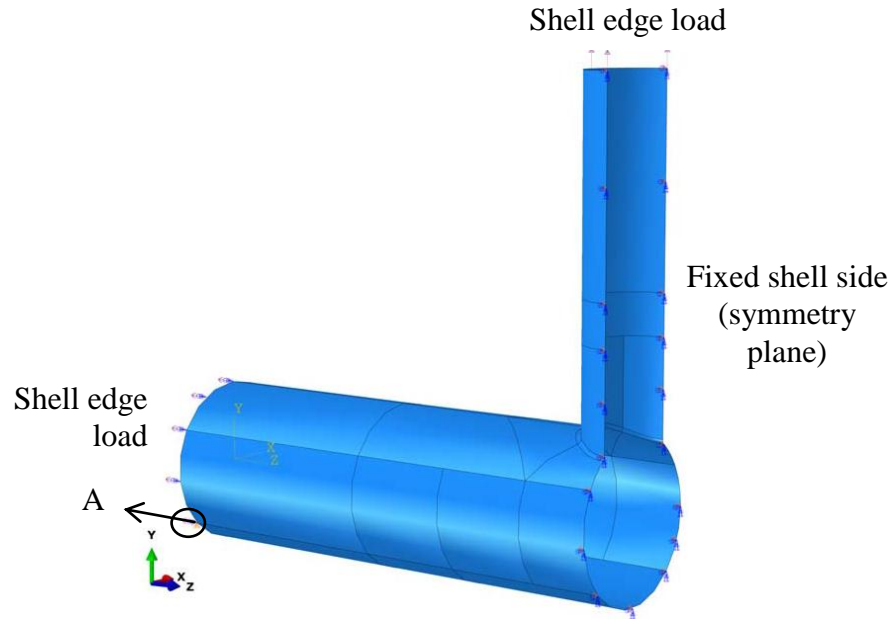


Figure 5: In-plane bending model boundary conditions





**Figure 6: Out-of-plane bending model boundary conditions**

In both figures, one edge of the run-pipe was fixed in the linear Z-direction, as the shell edge load was applied on the other end and on the end of branch also, to simulate the closed ended conditions in the run-pipe and the branch. Nodes “A” were fixed in the linear Y-direction to allow the run pipe to make circumferential deformation at the ends to simulate the long run-pipe to decrease the effect of the end conditions.

Elastic-plastic analysis was performed to get the limit in-plane or out-of-plane bending combined with pressure. The analysis was done in two numerical steps; the first was for the pressure only then the second was for the bending moment. In the load-deflection diagram (output of the analysis), readings of the deflection were taken to be the rotational displacement at the reference node that lies on the center point of the circular edge of the branch where the bending moment is applied, and it was plot versus the magnitude of moment load applied, as shown in Fig. 7

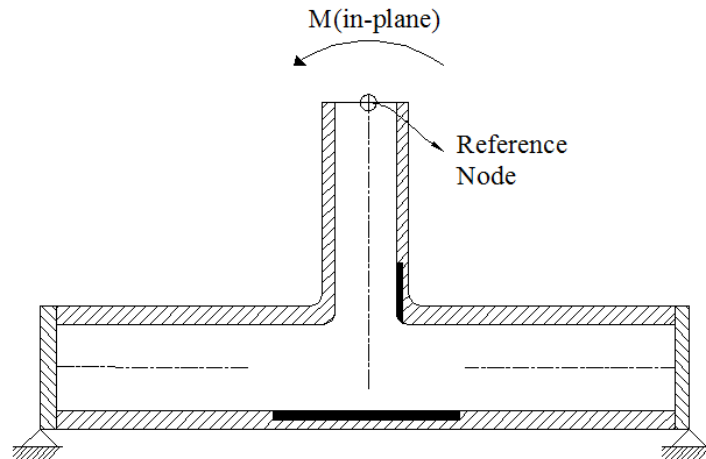


**Figure 7: Moment application and reference node**

## 2.5. *The existing API579 standard shakedown assessment procedures*

### 2.5.1. *The shakedown limit assessment procedure using an elastic-plastic analysis (API 579 standard)*

A direct application of lower bound shakedown theorem is to load and unload the component by a certain value and obtain the residual stresses generated after the unloading. When it reaches the yield limit, the corresponding load value is the shakedown limit, as shown in Fig. 8. This is called “Elastic-plastic ratcheting analysis” in API 579. This technique was used in this study as a verification of the Simplified Technique results as it shows the complete step framed behavior of the component whether in shakedown or ratcheting or reversed plasticity failure behavior.

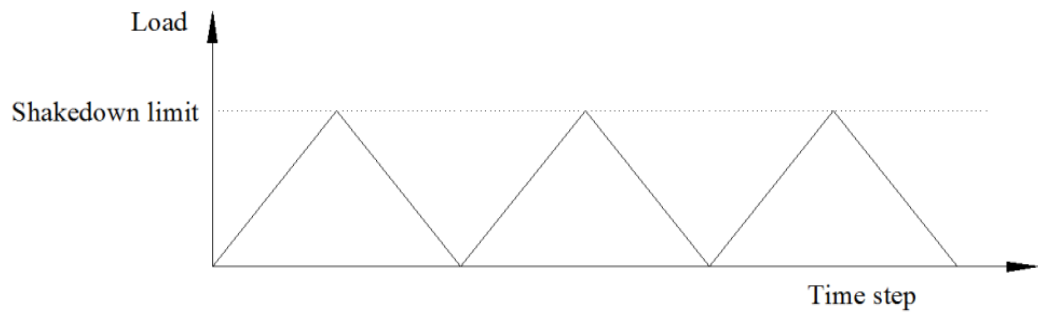


**Figure 8: Elastic-plastic shakedown analysis loading/unloading scheme (API 579)**

All results from the Simplified Technique were verified using a full cyclic elastic-plastic analysis with the same conditions for the same values obtained. The shakedown behavior was observed on stress-strain diagram (von Mises stress Vs. Equivalent plastic strain), and at higher bending moment values to observe the ratcheting and reversed plasticity behaviors.

As will be illustrated in results verification (chapter 5), in the shakedown situation, the stress-strain path during loading and unloading is expected to be without progressive plastic strain each cycle of loading. On the other hand, for the reversed plasticity behavior, there is a progressive plastic strain each cycle that alternates between tension and compression. When ratcheting occurs, some of points on the component experience progressive plastic strain in tension, and other points experience it in compression but it does not alternate from tension to compression or vice versa as the reversed plasticity.

### *2.5.2. The shakedown limit assessment procedure using an approximate elastic analysis (API 579 standard)*

For assessments that require approximate shakedown analysis, the design codes and API 579 included a simple elastic shakedown analysis that determines the shakedown limit without calculating the residual stresses in the system and without non-linear elastic-plastic analysis. It is based on the stress range when a uniaxial state of stress in a system is in shakedown. This range is from the yield in tension to the yield in compression equals to twice elastic limit ( $2\sigma_y$ ), as shown in Fig 9. Therefore, when the von Mises stress level hypothetically reaches the twice yield limit, the corresponding applied load is considered as the shakedown limit load, as shown in the equations 14 – 16 and Fig. 9.

The elastic analysis is just a linear elastic FE analysis for defected or sound components. It starts with application of any value of load to get the maximum von Mises stress in the component. Then by the lever rule using the input load, output stress and yield strength of the material and by assuming elastic-perfectly-plastic material model, the following limit (twice elastic limit) can be met and the shakedown load can be obtained.

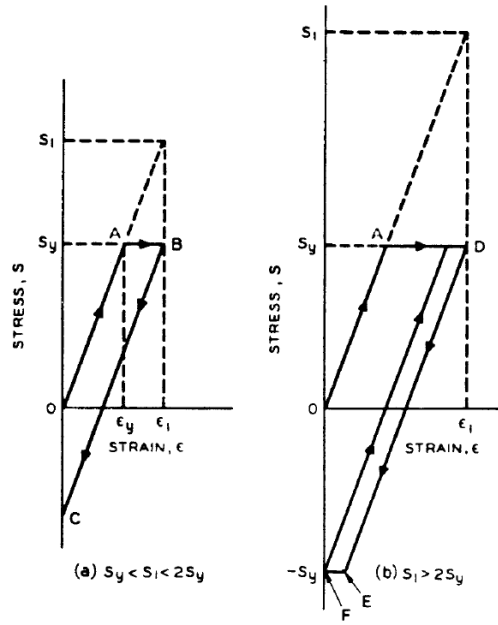


Figure 9: Elastic shakedown analysis [2]

$$\therefore \sigma_r = \sigma_y \quad \text{The shakedown limit condition by definition} \quad (15)$$

$$\therefore \sigma_e + \sigma_r = S_1 \quad \text{Elastic analysis} \quad (16)$$

$$\therefore S_1 = 2\sigma_y \quad \text{The shakedown limit load using elastic analysis} \quad (17)$$

## CHAPTER 3: MODEL VERIFICATION STUDIES

### 3.1. *First verification study: Limit load pressure of a straight tube with external wall thinning*

Before developing the complete model of locally thinned wall pipe-branch connection, local wall thinning modeling methodology was verified against experimental results. This is to build a reliable model that is ready to be used in limit and shakedown analyses using several assessment procedures. Moreover, the local wall thinning parameters are the main concern in this study and its well defined modeling is the key to validate the new assessment procedure.

Hui and Li [3] made hydrostatic tests on fixed and closed ended Inconel SG690 tubes with external rectangular local wall thinning at the mid span of the tube. These SG690 tubes were subjected to an internal pressure to plot it versus the radial deflection at the point of maximum displacement, which was found in the middle of the local wall thinning area, as shown in Fig. 10. Using Twice-Elastic Slope method the pressure limit load was determined.



Figure 10: Maximum strain at the middle of local wall thinning area, Hui and Li SG 690 tube experiment [3]

A quarter-model of the straight locally thinned wall tube was developed with the same geometry, loading, boundary conditions and local wall thinning parameters because of the double symmetry of the geometry and loading. The diameter was fixed to be 19.05 millimeter and the thickness 1.09 millimeter, as Hui and Li [5] chose to fix the diameter to thickness ratio variable to make all their tests on as shown in Fig.11.

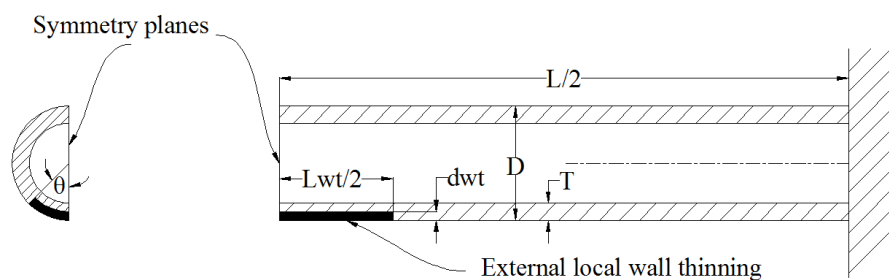


**Figure 11: Model of SG 690 straight tube with symmetry planes and local wall thinning area**

A shell element (S8R, ABAQUS CAE/STANDARD) and elastic-perfectly-plastic material were used with the same material properties of the SG 690 tube; yield limit of 309.8 MPa, Young's modulus of 211000 MPa and Poisson's ratio of 0.289 were used in the FE model. The local wall thinning area was defined as a separate S8R region of elements that has a thinner thickness than the rest of tube, as shown in Fig.12.

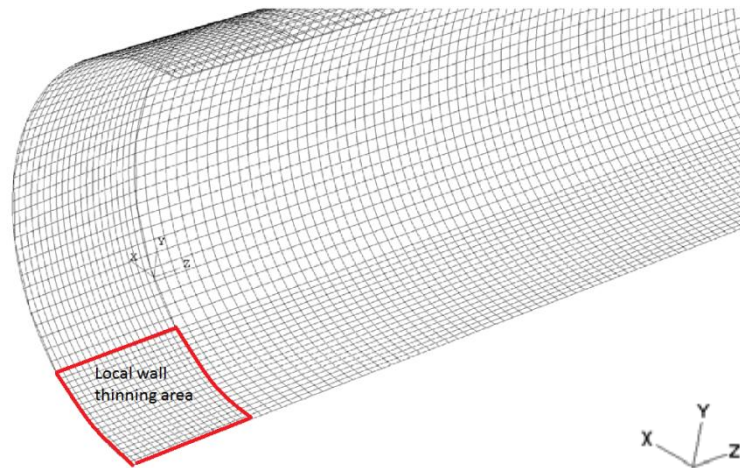


**Figure 12: Typical mesh of quarter-model for SG 690 straight tube with external local wall thinning region**

Two specimens were chosen to be compared with the numerical results of the model. For specimen (1) that had a rectangular local wall thinning of depth of 39.3% of the total thickness, the limit pressure was found to be 29.21 MPa experimentally as shown in Fig. 13, and 29.6 MPa numerically as shown in Fig. 14.

As shown in Table 2, although the material model of the numerical analysis assumed that there is no strain hardening in the material (elastic-perfectly-plastic material model), both results (numerical and experimental) are almost the same with a minimal discrepancy. It means that the strain did not go into plastic range as much as to make large discrepancy between the two material models.



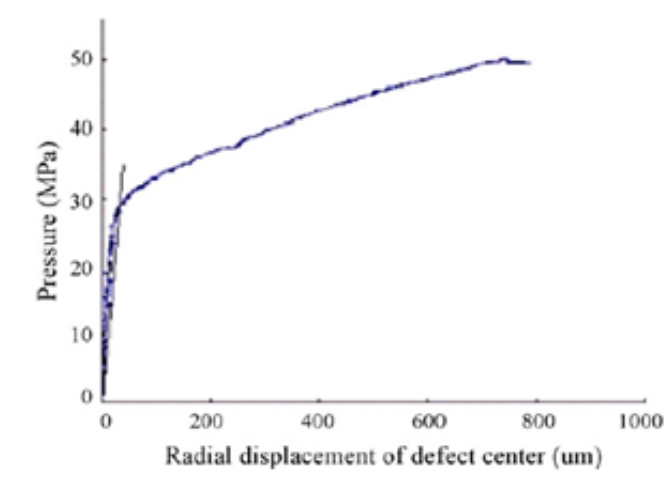


Figure 13: Load-Deflection diagram of Hui and Li experiment (specimen. 1) [3]

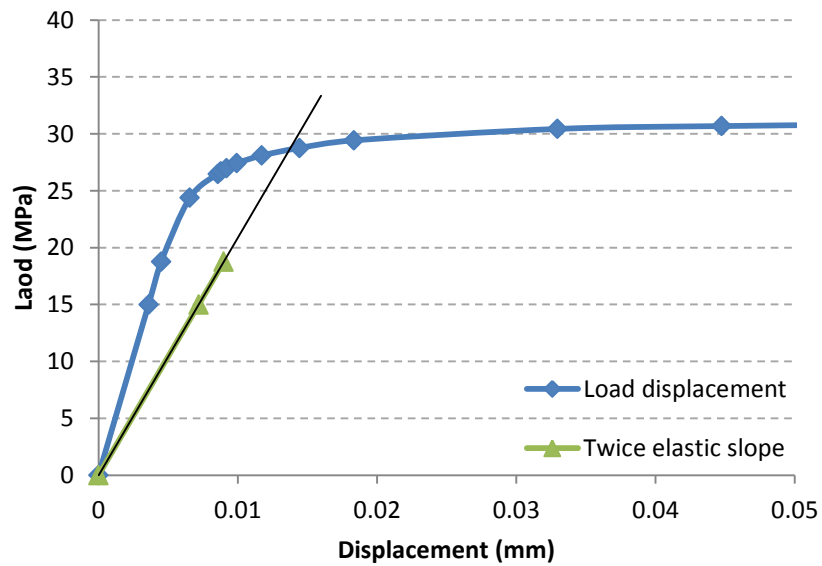


Figure 14: Twice-Elastic Slope method on load-deflection diagram of the FE model (specimen. 1)

Table 2: Comparison of the results of a straight locally thinned wall tube (verification study. 1)

Specimen number	Local wall thinning depth to thickness ratio (%)	Experimental Limit Pressure (MPa)	Numerical FE Limit Pressure (MPa)	Discrepancy (%)
1	39.3	29.21	29.6	1.33
2	42.1	27.85	27.3	1.97

From the previous comparison, the results of the numerical model agreed well with the experimental results as the maximum error is less than 2% using the same limit load determination technique (Twice-Elastic Slope method). Therefore, the FE modeling methodology of the local wall thinning was verified and applicable to be added in the model of the branch-pipe connection.

### ***3.2. Second verification study: Limit pressure of locally thinned wall pipe-branch connection***

Lee et al. [14] developed a numerical model for the previously illustrated pipe-branch connection (section 2.4.) for two locations of local wall thinning, on the branch next to the intersection and on the run-pipe opposite to the branch. A limit pressure was obtained using a twenty-node iso-parametric, reduced integrations quadratic brick element (C3D20R, ABAQUS/STANDARD) with minimum six elements through the thickness. An elastic-perfectly-plastic material model was used with Riks option to avoid problems of convergence. The solution covered a wide range of pipe-branch connection sizes, branch to run-pipe radius and thickness ( $r/R = t/T \leq 1$ ) and mean radius to thickness ratio  $5 \leq R/T \leq 20$ . For the defect size, the solution covered local wall thinning depth  $0.3 \leq d_{wt}/t \leq 0.7$ , local wall thinning axial length  $0 \leq L_{wt}/R \leq 10$  for local wall thinning on the run-pipe and  $0 \leq L_{wt}/r \leq 6$  for local wall thinning on the branch.

The same previously verified methodology of modeling was used to develop a locally thinned wall pipe-branch connection with geometrical and local wall thinning parameters from the model developed by Lee et al. [14]. Pressure was applied and

load-deflection diagram was plot to obtain the limit pressure for the component and compare it with numerical results of Lee et al. [14].

As in the first verification study, the model was developed using a quadratic 8-node shell element (S8R, ABAQUS CAE/STANDARD) and elastic-perfectly-plastic material model. Two local wall-thinned pipe-branch connection models were developed; a quarter-model due to the double symmetry in the geometry and loading when the local wall thinning lied on the run-pipe, and half-model when the local wall thinning lied on the branch next to the intersection line, as shown in Fig. 15. The intersection between branch and run pipe was modeled with a minimal fillet (equals to the minimum thickness) to avoid stress concentration.

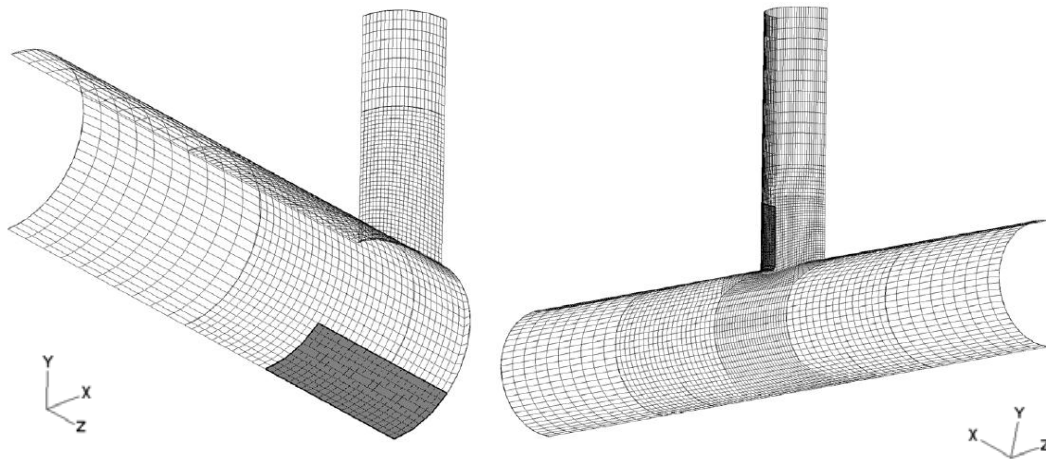


**Figure 15: Quarter and half models used in the 2nd verification study; shaded regions are the local wall thinning areas**

Results showed good agreement with Lee et al. [14] results with acceptable discrepancy, as shown in Table 3. For example in case (1), the local wall thinning depth to total thickness ratio ( $d_{wt}/t$ ) of 0.7 and length of the local wall thinning over

radius ratio ( $L_{wt}/R$ ) of 0.5, using Twice-Elastic Slope method in the load-deflection diagram as shown in Fig. 16, the limit pressure was found to be 13.6 MPa while result of Lee et al. [14] was 14.5 MPa.

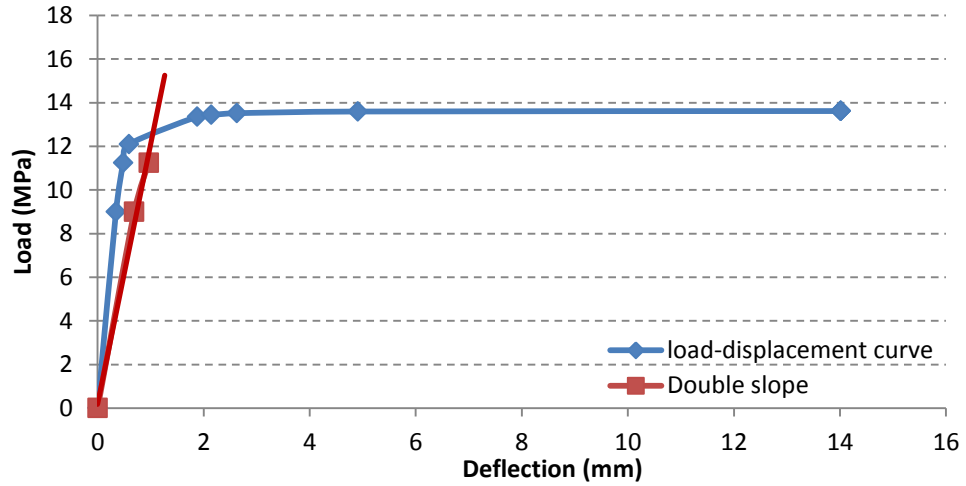


Figure 16: Limit pressure using Twice-Elastic Slope (case 1)

Table 3: Comparison of the results of locally thinned wall pipe-branch connection limit pressure (verification study 2)

Case #	$L_{wt}/R$	$d_{wt}/t$	The model limit pressure	Lee et al. limit pressure	Discrepancy %
1	0.5	0.7	13.6	14.5	6
2	4	0.5	17.4	18	3.3
3	4	0.7	10.41	10.4	0.09

### ***3.3. Verification of the model of locally thinned wall pipe-branch connection using API 579 standard limit pressure assessment procedures***

#### ***3.3.1. Area replacement method***

Area replacement method can be applied on unreinforced or reinforced nozzles and pipe-branch connections. A requirement to apply area replacement method in API 579 is to have a strain hardening material of Yield strength/ Ultimate strength=0.8. Therefore, a bilinear material model was used, that has Yield strength/ Ultimate strength=0.8 and plastic strain of 0.2 corresponding to the ultimate stress. Area replacement method does not include bending moments applied and it also does not evaluate the local wall thinning effect when it lies on the run-pipe opposite to the intersection. Therefore, it was applied to compare the limit pressure for the previously modeled pipe-branch connection when the local wall thinning lied on the branch only.

Area replacement method equations are based on a compensation of the cut projected area due to branch connection by means of areas available in reinforcement, branch thickness, run-pipe thickness, etc. Therefore, the available areas in the pipe-branch connection should be equal to or greater than the required area.

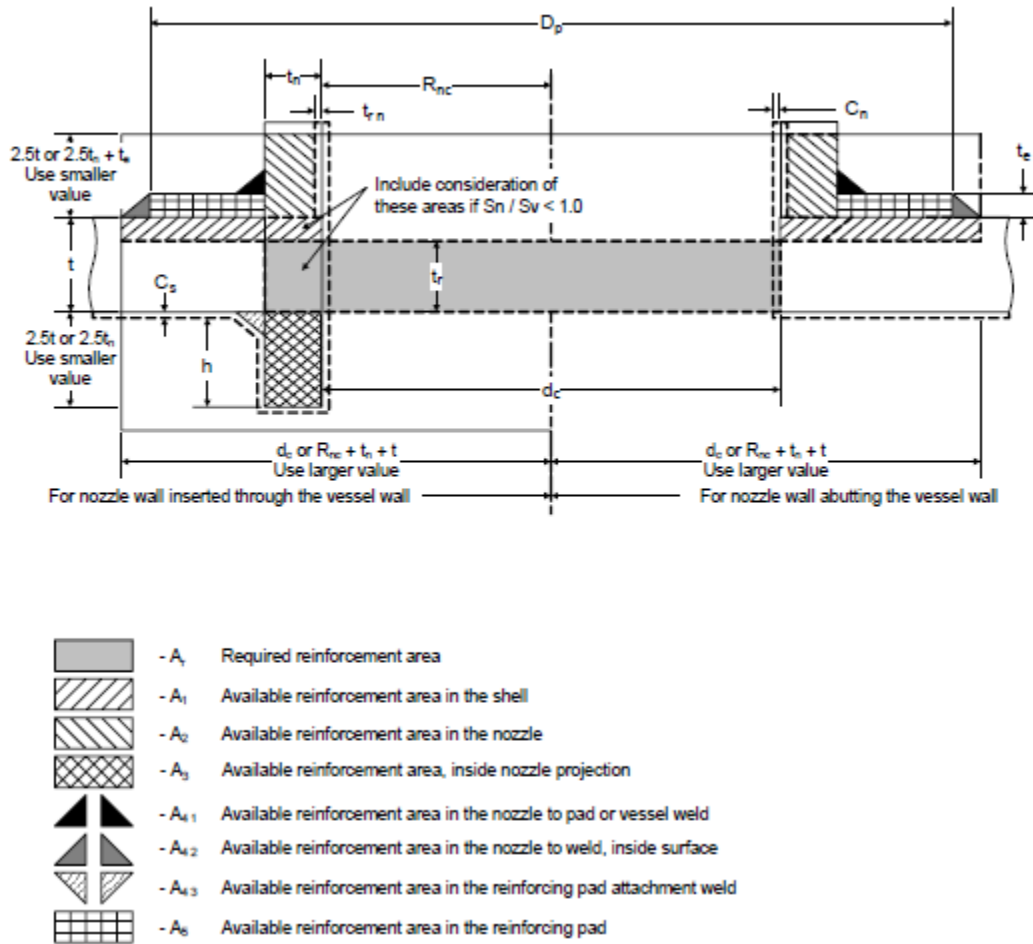


Figure 17: Typical pipe-branch connection areas for Area Replacement Method of API 579 [4]

In the concerned pipe-branch connection, an ideal case of geometry was selected (section 2.4.1). All welds are not considered in the pipe-branch connection ( $A_{41}=A_{42}=A_{43}=\text{zero}$ ). There is no reinforcing pad ( $A_5=\text{zero}$ ), and no inside nozzle projection ( $A_3=\text{zero}$ ). Therefore, in the pipe-branch connection concerned in this comparison, the available areas in the shell (run-pipe) and nozzle (branch pipe) should be equal or greater than the required area. The original equations of the area replacement method were simplified to the concerned pipe-branch connection to lead to the equations (17-20).

Also, there are factors in the area replacement method's original equations valued by zero or one according to its definition and application to the concerned

simple geometry of the pipe-branch connection, as shown in Table 4. All definitions are in the nomenclature section of the thesis.

**Table 4: Area replacement method variables' selected values**

Variable	value	Remarks
F	1	No axial force
$f_{r1}$	1	Set-on nozzle
$f_{r2}$	1	Same material considered for both branch and run pipes
$E_1$	1	Ideal joint efficiency
$J_r$	1	No external pressure
$w_h$	0	No weld leg on the inside surface of the run-pipe
$h$	0	No elliptical head from the inside surface of the run-pipe
$C_s$	0	No local wall thinning on the run-pipe next to the intersection

$$A_r = d_c t_r \quad (18)$$

$$A_1 = \max. \left\{ \begin{array}{l} d_c(T - T_r) \\ 2(T + t - d_{wt})(T - T_r) \end{array} \right. \quad (19)$$

$$A_2 = \min. \left\{ \begin{array}{l} 5T(t - d_{wt} - t_r) \\ 5(t - d_{wt} - t_r)(t - d_{wt}) \end{array} \right. \quad (20)$$

$$A_r \leq A_1 + A_2 \quad (21)$$

The previously discussed quarter FE model in the limit pressure of locally thinned wall pipe-branch connection (second verification study) was used. A limit pressure analysis was performed based on Twice-Elastic Slope method for the previously selected pipe-branch connection. Limit pressures were determined for a range of local wall thinning depth to total thickness ratio of 0-0.7. The material model used in this analysis is a bi-linear elastic-plastic model with Yield over Ultimate strength ratio of 0.8, and plastic strain of 0.2 corresponds to the ultimate strength

value. Then the limit pressure was plot against area replacement method results for the same geometry and local wall thinning configurations, as shown in Fig. 18.

An example will be illustrated of how the area replacement method was applied. For the same geometrical parameters selected in section 2.4.1, the run-pipe thickness  $T=4$  millimeter, branch thickness  $t=2.4$  millimeter and diameter of the circular opening (branch inside diameter plus local wall thinning depth)  $d_c=73.2$  millimeter. For the local wall thinning depth  $d_{wt}= 0.6$  millimeter. The available area from the run-pipe ( $A_1$ ) was determined to be  $144 \text{ mm}^2$  from equation 18, and the available area from the branch ( $A_2$ ) was determined to be  $5.5 \text{ mm}^2$  from equation 19. Therefore, the required area was determined to be  $149.5 \text{ mm}^2$ . Finally, the limit pressure was generated from the required thickness ( $t_r$ ) to be  $14.8 \text{ MPa}$  and normalized to be  $0.5$ , as shown in Fig. 18.

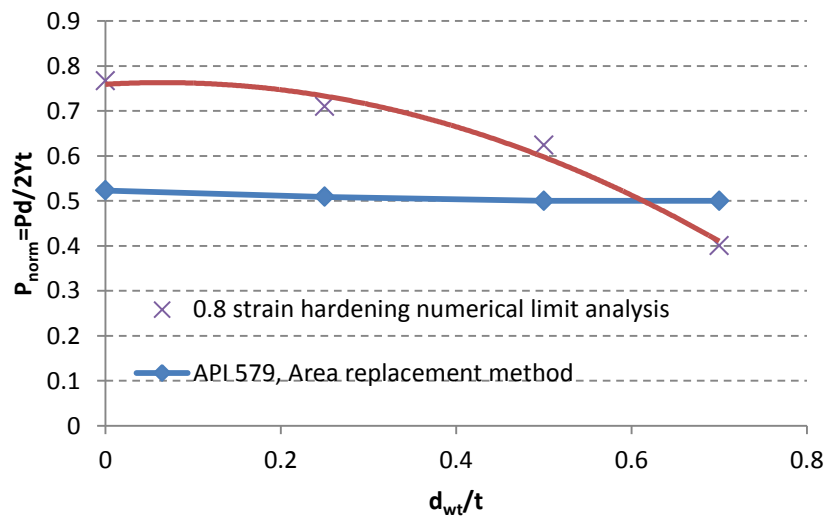


Figure 18: Comparison of the limit pressure for API 579 and numerical analyses while changing the local wall thinning depth



Area replacement method showed conservative results as noted in API 579 standard. On the other hand, it did not show sufficient decrease of the limit load with the increase of the depth of the local wall thinning, as the numerical models showed, although it lies in the most critical stress concentrated area –on the intersection between run and branch pipes. Moreover, the limit load does not depend on the local wall thinning area, especially the circumferential length, as it is not found as a variable in the equations.

### 3.3.2. *Limit analysis method*

In limit analysis procedure, nozzle-vessel intersections and pipe-branch connections can be assessed only when they do not have a reinforcement pad. As noted in API 579 standard, the limit analysis method can determine the limit pressure with acceptable accuracy, less conservative than area replacement method. On the other hand, it has several limitations concerned with the location of local wall thinning, material strain hardening, nominal pipe size, operating temperature, and applied loadings. Therefore, the verification model was required to be built using the bi-linear elastic-plastic including strain hardening (Yield strength/ Ultimate strength=0.8) material model that is previously mentioned in the area replacement method. The local wall thinning location considered is on the branch next to the intersection case only. In other words, as the limitations did not add any additional requirements for the concerned pipe-branch connection, the FE model of previous area replacement method was typically used to conduct this verification study.

The limit analysis method's equations are a typical curve fitting of numerical limit pressure analysis. Therefore, using the geometrical and local wall thinning parameters used in area replacement method, the equations can be satisfied.

For the selected geometry and loading of the concerned pipe-branch connection, the parameters of the limit analysis method were determined. Local wall thinning value on run pipe ( $C_s$ ) equals to zero as the local wall thinning only located on the branch. A and B values were determined to be 162 and 210 respectively from the thickness of run and branch pipes and local wall thinning depth values. Other geometrical parameters were selected as mentioned in Table 1.

The following limit analysis method equations (21) and (22) were satisfied to get the limit pressure for the previously modeled pipe-branch connection. As the Local wall thinning depth was the only variable concerned in this study ( $C_n$ ), a graph of limit pressure versus the local wall thinning depth to total thickness ratio was plot to compare the results of the numerical model with area replacement method and this procedure, as shown in Fig. 19. The limit pressure was normalized to a straight pipe limit pressure as shown in section 2.4.1.

$$\frac{2+2\left(\frac{d_m}{D_m}\right)^{3/2}\left(\frac{t_n-C_n}{t-C_s}\right)^{1/2}+1.25\lambda}{1+\left(\frac{d_m}{D_m}\right)^{1/2}\left(\frac{t_n-C_n}{t-C_s}\right)^{3/2}} \leq 2.95 \left(\frac{t-C_s}{t_r}\right) \quad (22)$$

$$\frac{\lambda\left[A\left(\frac{t_n-C_n}{t-C_s}\right)^2+228\left(\frac{t_n-C_n}{t-C_s}\right)\left(\frac{d_m}{D_m}\right)+B\right]+155}{108\lambda^2+\lambda\left[228\left(\frac{d_m}{D_m}\right)^2+228\right]+152} \geq (0.93+0.005\lambda) \left(\frac{t_r}{t-C_s}\right) \quad (23)$$

Where  $\lambda$ , A and B are parameters can be determined using the following equations,

$$\lambda = \left( \frac{d_m}{D_m} \right) \sqrt{\frac{D_m}{t - C_s}}$$

$$A = 162 \quad \text{for} \quad \left( \frac{t_n - C_n}{t - C_s} \right) \leq 1$$

$$B = 210 \quad \text{for} \quad \left( \frac{t_n - C_n}{t - C_s} \right) \leq 1$$

$$A = 54 \quad \text{for} \quad \left( \frac{t_n - C_n}{t - C_s} \right) > 1$$

$$B = 318 \quad \text{for} \quad \left( \frac{t_n - C_n}{t - C_s} \right) > 1$$

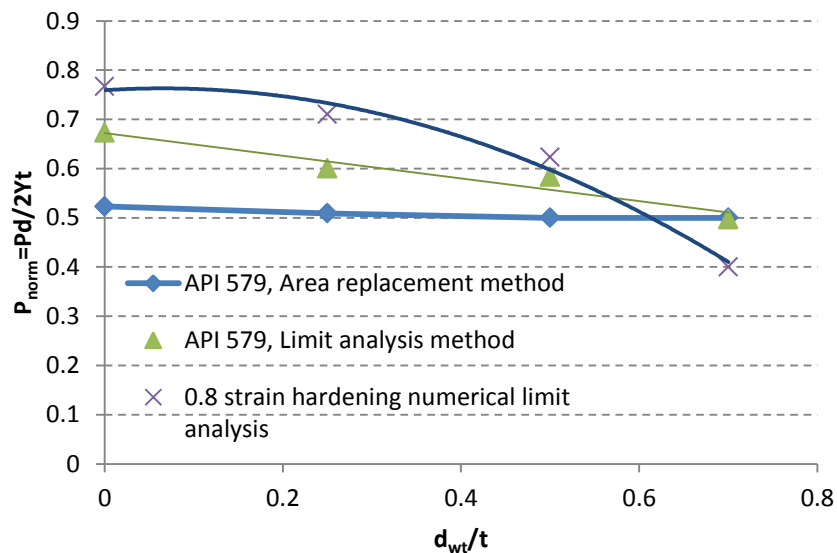


**Figure 19: Comparison of results of area replacement method vs. limit analysis method vs. developed FE model**

A case is selected for illustration of how the limit analysis method was applied in the concerned pipe-branch connection. For the same geometrical parameters selected in section 2.4.1, the run-pipe thickness  $T=4$  millimeter, branch thickness  $t=2.4$  millimeter and diameter of the circular opening (branch inside diameter plus

local wall thinning depth)  $d_c=73.2$  millimeter. For the local wall thinning depth  $d_{wt}=0.6$  millimeter. Parameters were determined from their equations,  $\lambda=2.615$ ,  $A=162$  and  $B=210$ . The required thickness ( $t_r$ ) was determined from the equations 21 and 22 to be 2.36 millimeter. Therefore, the limit pressure was determined from the required thickness to be 18 MPa and normalized to be 0.6 as shown in Fig. 19.

From Fig. 19, the limit analysis method showed a linear decrease in limit pressure with the increase of local wall thinning depth and close to the numerical model. On the other hand, the area replacement method does not respond to the increase of the local wall thinning depth but it has a conservative result that corresponds to the minimum value reached by the limit analysis method. This is what API 579 standard means by conservative results generated from the area replacement method. This is valid till the start of the range  $0.6-0.7 d_{wt}/t$ , approximations in the equations of the two methods lead to higher values than the numerical results.

## CHAPTER 4: RESULTS AND DISCUSSION

### 4.1. *Limit load analysis*

In previous chapters, limit pressure analyses were conducted to the locally thinned wall pipe-branch connection model for the purpose of verification. The limit analyses results were compared to Lee et al. [14] FE model results. Then, the results were compared to API 579 standard limit pressure assessment procedures. Thus, the FE model is now verified to conduct limit moment analyses in the presence of pressure, to show the effect of local wall thinning depth and location on the limit moment, and the most critical locations of local wall thinning.

The limit moment was determined using the Twice-Elastic Slope method from the curves of moment versus rotational displacement of the reference node. For example, a case when local wall thinning lies on the branch next to the intersection with  $d_{wt}/t$  ratio of 0.5. The objective is to determine the limit of in-plane bending moment applied on the branch in the presence of internal pressure of 3 MPa, as shown in Fig. 20. Finally, the pressure and moment limits are normalized to the limit pressure ( $P_{norm}$ ) and limit moment ( $M_{norm}$ ) of a straight pipe as illustrated in section 2.4.1. The geometry and local wall thinning configurations were used as in chapter 3 - Table 1. Twice-Elastic Slope was applied to get the limit moment from the moment vs. rotational displacement diagram, as shown in Fig. 21.

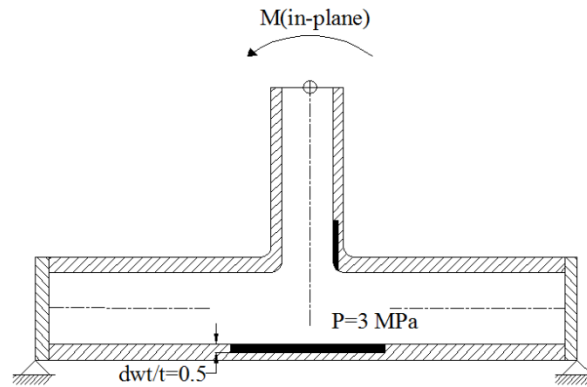


**Figure 20: Limit in-plane moment with the presence of 3 MPa pressure and 0.5  $d_{wt}/t$  ratio**

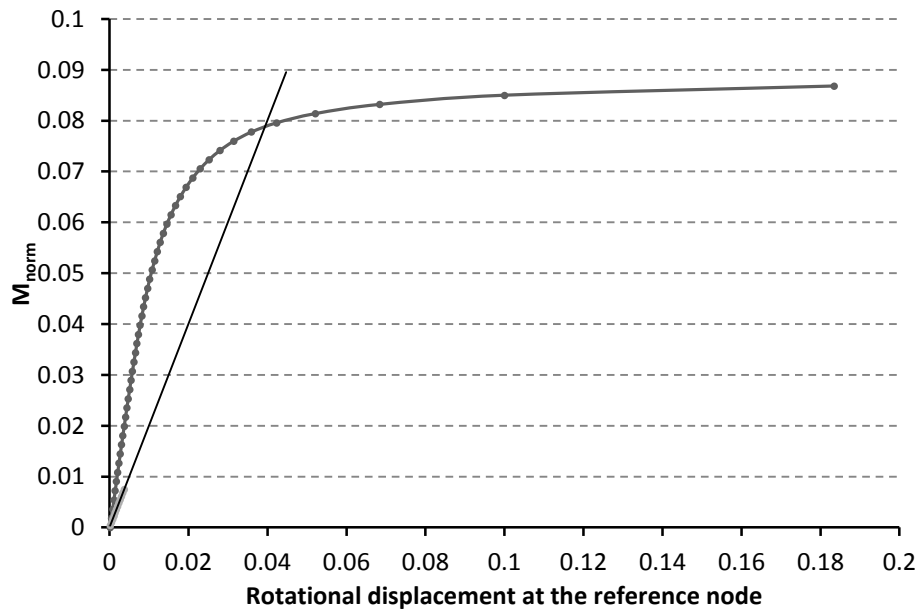


**Figure 21: Limit moment determination using Twice-Elastic Slope method in moment vs. rotational disp. Diagram**

The previous limit moment analysis was conducted for the full acceptable pressure range (from zero till the limit pressure for the component) to construct the limit moment boundary curve. The following sections will illustrate the limit moment boundary to show the effect of the local wall thinning depth and location and loading type.

#### 4.1.1. Limit load analysis for sound pipe-branch connections

As shown in Fig. 22, the limit boundary of out-of-plane moment for a sound pipe-branch connection was determined and compared with Tabone and Mallette [13] simplified formula (equation 23). This proves that the limit moment boundary can be determined using the values of  $P_{SL}$  and  $M_{SL}$  (the limit load value of the corresponding single load situation) as it is an elliptical curve connecting the two values as in Tabone and Mallette formula.

$$\left(\frac{P}{P_{SL}}\right)^2 + \left(\frac{M}{M_{SL}}\right)^2 = 1 \quad (24)$$

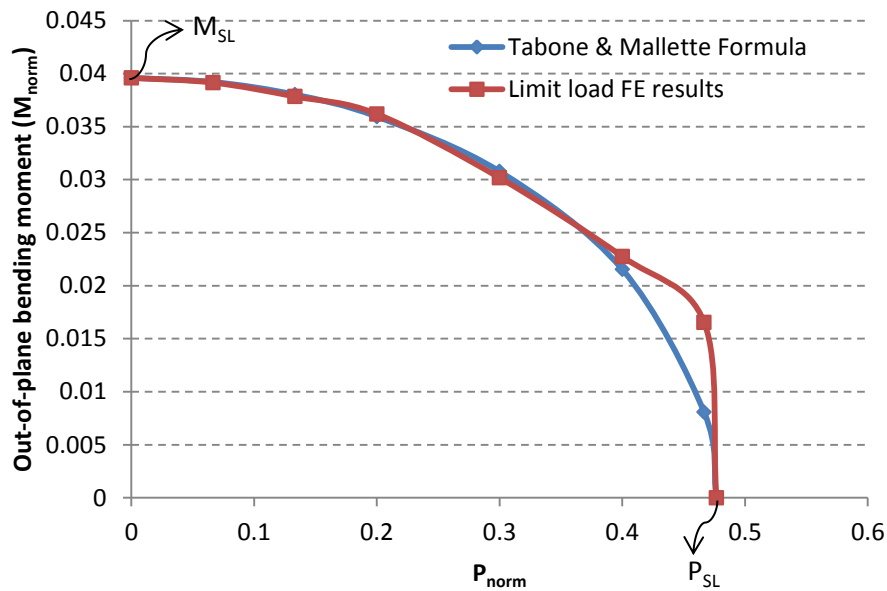


**Figure 22: Comparison of the limit boundary of out-of-plane moment with Tabone and Mallette formula**

For the in-plane bending moment situation, the limit moment boundary showed the same elliptical curve, as shown in Fig. 23. It was compared to Xuan et al. [11] who obtained the same curve for in-plane bending using a numerical analysis for a sound pipe-branch connection having the same  $d/D$  ratio of 0.6. The two results

showed some discrepancies because of the load incrementing included in the numerical analyses.

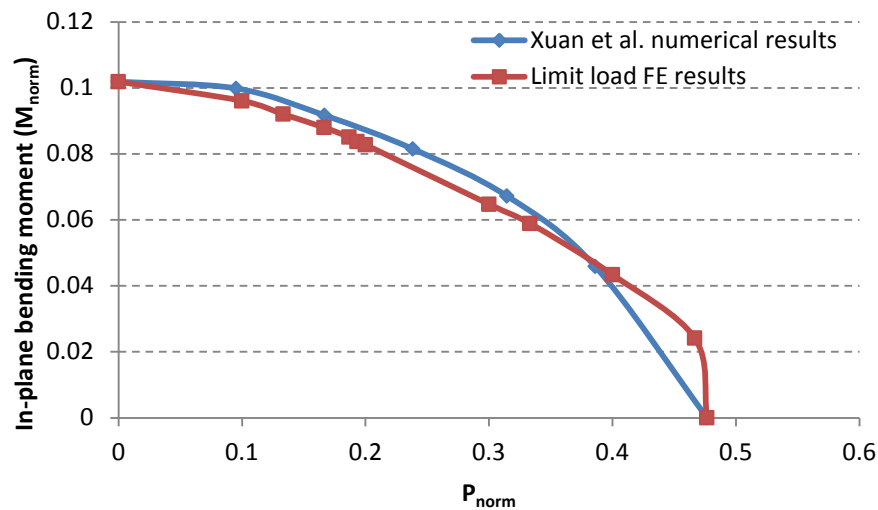


**Figure 23: Comparison of the limit boundary of in-plane moment with Xuan et al. numerical results**

#### 4.1.2. Limit load analysis for locally thinned wall pipe-branch connections

As discussed in the previous sections, local wall thinning locations considered in this study are on the branch next to the intersection and on the run-pipe opposite to the branch. These locations are the most critical for the possible flow directions. The results of the limit load analysis are discussed according to the location of the local wall thinning, as will be shown in the following sections.

##### 4.1.2.1. Limit load results when the local wall thinning lies on the run-pipe opposite to the branch-pipe

For the case of local wall thinning lies on the run-pipe, the boundary curves have a decreasing limit moment that plots the same elliptical curve made by Tabone and Mallette [13] and Xuan et al. [11], as shown in Figs. 24 and 25. This is because



the local wall thinning does not have a severe geometrical effect to change the overall shape of the limit load boundary curve for the component.

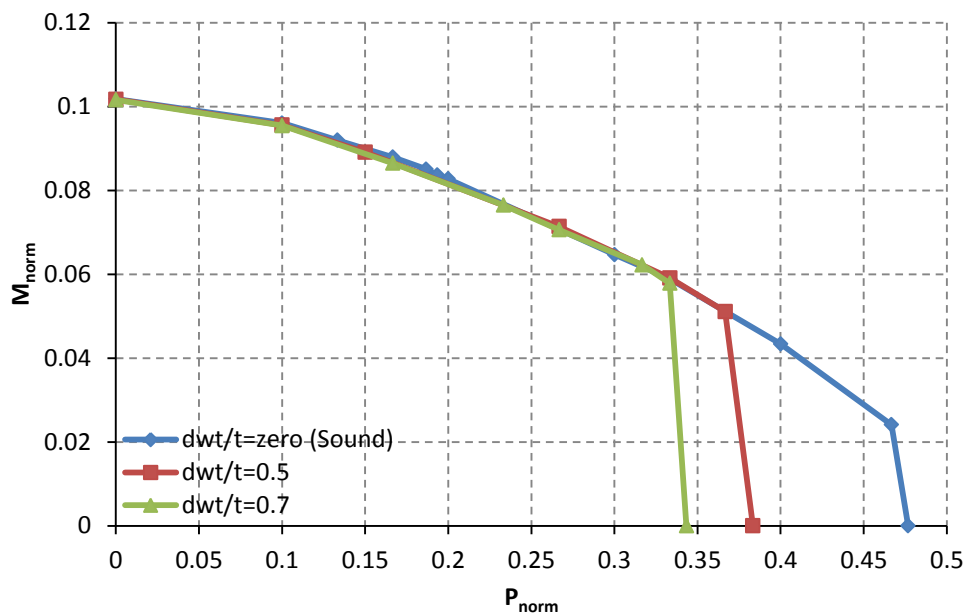


Figure 24: In-plane moment limit boundary when the local wall thinning lies on the run-pipe

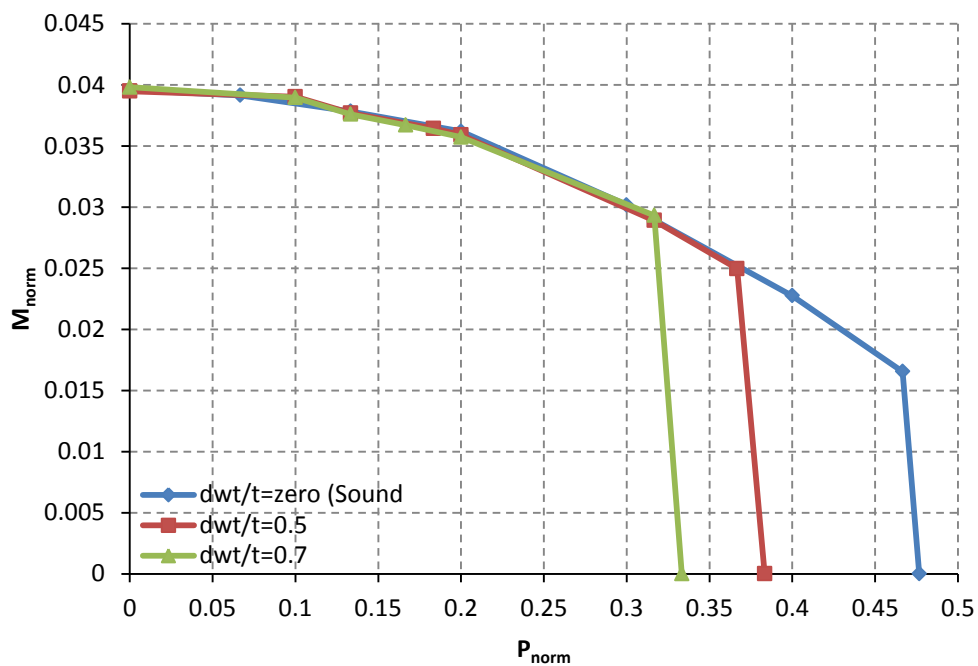


Figure 25: Out-of-plane moment limit boundary when the local wall thinning lies on the run-pipe

The effect of the local wall thinning can appear in the pressure limit, as it decreases with the increase of local wall thinning depth. The pressure limit complied with equation (24) of the pressure limit of a straight pipe with the minimum thickness at the locally thinned wall region.

$$P_{SL} = 2Yt_{min}/d \quad (25)$$

The elliptical curves drop to zero directly once the limit pressure is reached, as shown in Figs. 24 and 25. The limit moment has the same values for all local wall thinning depths. This effect can be because of the location of the local wall thinning on the run pipe at zero internal reaction moment, as shown in the bending moment diagram for the simply supported run pipe in Fig. 26.

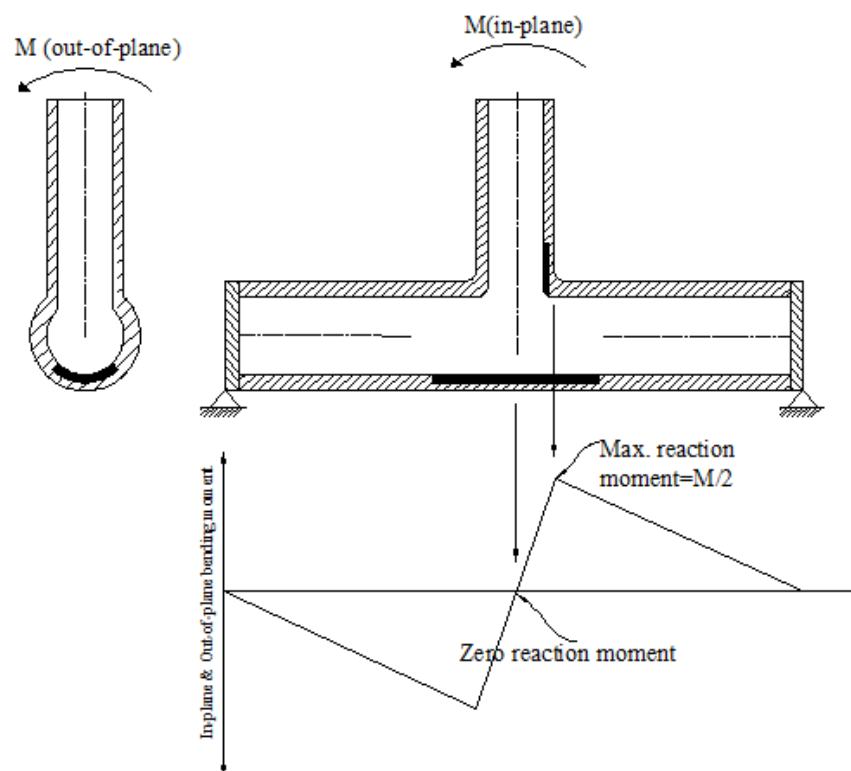


Figure 26: Bending moment diagram a pipe-branch connection when it is subjected to bending moment on the branch

4.1.2.2. *Limit load results when the local wall thinning lies on the branch next to the intersection*

For the case of local wall thinning lies on the branch next to the intersection, the limit moment boundary curves support the point of having the same elliptical curves of Tabone and Mallette [13] and Xuan et al. [11] for out-of-plane and in-plane bending moments respectively, as shown in Figs. 27 and 28. Boundary curves also supports the point of wherever the local wall thinning lies, the elliptical shape of the limit load boundary curve is found, as there is no major geometrical change in the component, and so the limit load boundary.

Therefore, these exact parallel curves showed that the Tabone and Mallette [13] simplified formula and results of Xuan et al. [11] are also applicable for locally thinned wall pipe-branch connection. The moment and pressure limits used in Tabone and Mallette formula (equation 23) can be obtained when they are applied solely with the presence of the targeted local wall thinning in the pipe-branch connection ( $P_{SL}$  and  $M_{SL}$ ), then the whole curve can be obtained.

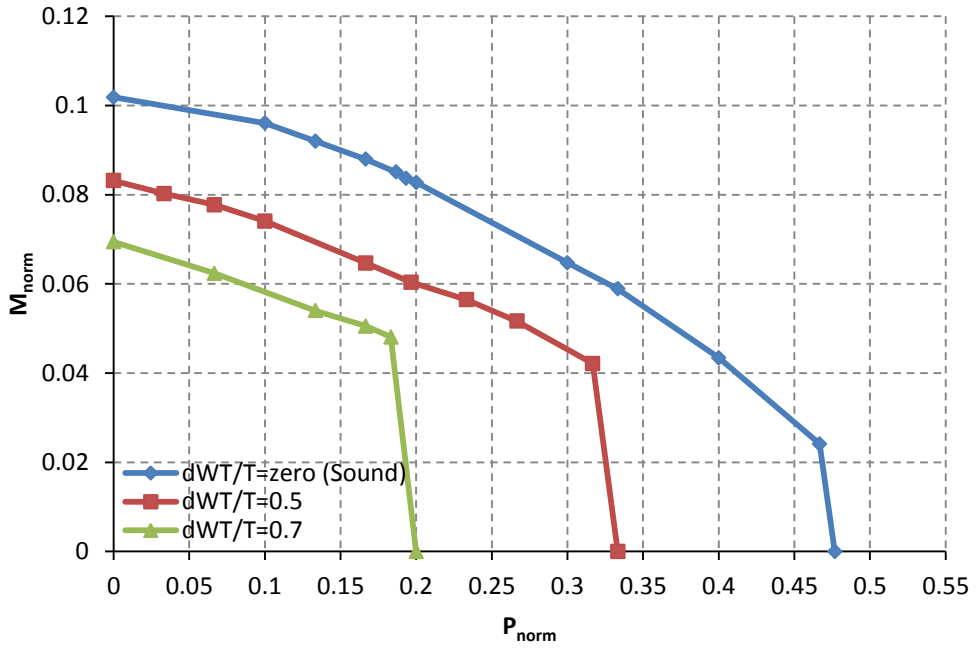


Figure 27: In-plane moment limit boundary when the local wall thinning lies on the branch

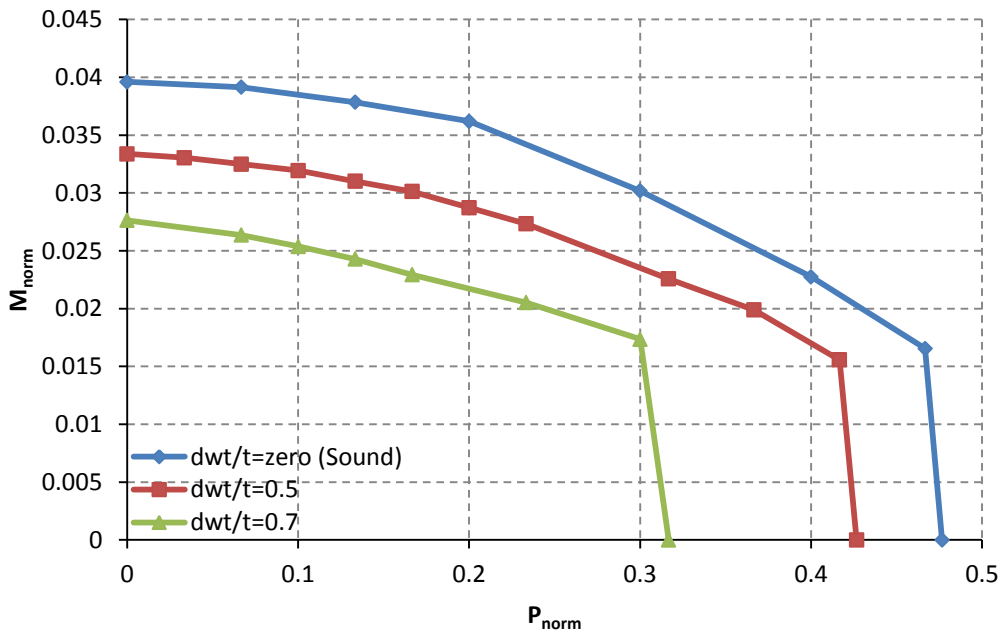


Figure 28: Out-of-plane moment limit boundary when the local wall thinning lies on the branch

Unlike the case of local wall thinning lies on the run pipe, both moment and pressure limits decrease as  $d_{wt}/t$  ratio increases to plot parallel curves. This is because

the local wall thinning lies on the most critical section of the component, at the maximum reaction moment in the bending moment diagram, as shown in Fig. 26.

As shown in Figs. 27 and 28, the limit moment boundary drops to zero earlier, in pressure rating, than the local wall thinning that lies on the run pipe. This is because the local wall thinning depth has a higher effect on the limit pressure, when it lies on the branch next to the intersection that is an area of stress concentration.

#### 4.2. *Shakedown limit load analysis*

By recalling the objectives of this study, the main results are the shakedown limit boundary of the locally thinned wall pipe-branch connection subjected to steady pressure and cyclic bending moment. It is the main concern in the verification process. Therefore, a major part in this research is to generate these results and compare it with solutions of the existing assessment procedures in API 579 standard, and finally to show the value added by the proposed assessment procedure to API 579 standard based on these comparisons.

Similar to the previous limit load analysis, a shakedown limit boundary curves (in shakedown analysis is called Bree diagram) was constructed using series of shakedown analyses for the whole acceptable pressure range. The Bree diagram was constructed for every local wall thinning depth, 0 (sound), 0.5 and 0.7  $d_{wt}/t$  ratios, and location and every bending moment direction. For example, to plot a Bree diagram for a pipe-branch connection including local wall thinning that lies on the run-pipe of 0.5  $d_{wt}/t$  ratio, as shown in Fig. 29. An internal pressure of 0.1 (normalized value) was applied and cyclic in-plane bending moment of 0.1 (normalized value) was applied on the branch. An elastic analysis was conducted for the case to obtain the elastic limit load that has a normalized value of 0.02. Then, an elastic-plastic analysis was conducted to obtain the limit moment that has a normalized value of 0.098. Finally, the Simplified Technique was applied using the previous two analyses, as in equation(25).

$$\sigma_{r_i} = \sigma_{ELPL_i} - \sigma_E \frac{M_i}{M_{ref}} \quad (26)$$

The shakedown limit moment is the load increment  $M_i$  that corresponds to residual stresses  $\sigma_{r_i}$  equals to the yield limit in elastic perfectly-plastic material model. As a result, the shakedown limit moment in this case was obtained to have a normalized value of 0.06.

This previous procedure was applied for the whole acceptable pressure range,  $0 \leq P \leq 0.186$  in this case. This pressure range did not reach the limit pressure of normalized value of 0.383. It reached a pressure value that when to apply any minimal value of bending moment, it leads to residual stresses that have the yield limit value. This means that the plotted shakedown moment value in the Bree diagram tends to zero. In other words, any cyclic load leads to ratcheting failure when this value of pressure is applied. Therefore, this value of pressure can be noted as shakedown pressure ( $P_{SD}$ ) even if it is already a steady load.

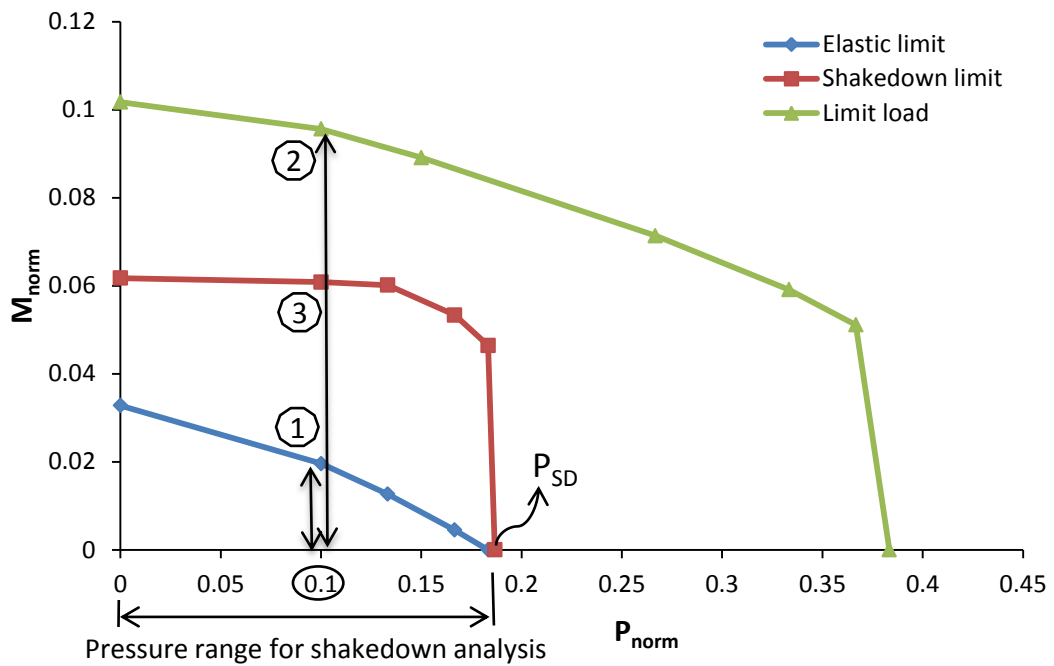


**Figure 29: Bree diagram of a pipe-branch connection with 0.5  $d_{wt}/t$  local wall thinning and subjected to in-plane bending**

As shown in Fig. 29, the three boundaries of elastic, shakedown and limit load create a three major zones; Elastic zone, where no plasticity can be found and it is used extensively by design codes; Shakedown zone, where the component experiences some plastic deformations in the first cycles of loading, but not major changes in its dimension, the plastic strain stabilizes as the stresses fluctuate in the elastic stress range again as in the elastic zone; Limit load zone, where the component is not safe except when it is subjected to steady loads only, it means that any cyclic loads will cause failure. In fact, the shakedown Bree diagram for the sound pipe-branch connection  $-d_{wt}/t$  ratio equals zero- already matches the Bree diagram of Abdalla et al. [24] exactly as it was generated using the same Simplified Technique.



#### 4.2.1. The shakedown limit boundary curves

For the purpose of comparison and discussion, the shakedown Bree diagrams were combined to show the effect of the local wall thinning depth and location on the shakedown boundaries only.

When the shakedown limit boundary was plot, it typically showed two ranges; the plateau (range "A"), where it starts from zero-pressure till a certain value of pressure, as shown in Fig. 30. Full cyclic elastic-plastic FE analyses were conducted on values just above this curve of this range. It was found that it has a reversed plasticity failure behavior. The results of the full cyclic elastic-plastic FE analysis will be discussed intensively later in chapter 5.

The inclined range "B", it starts from the end of the plateau till shakedown limit pressure ( $P_{SD}$ ). It was found from the same analysis for the values just above the curve and beyond the  $P_{SD}$  limit that both have ratcheting failure behavior.

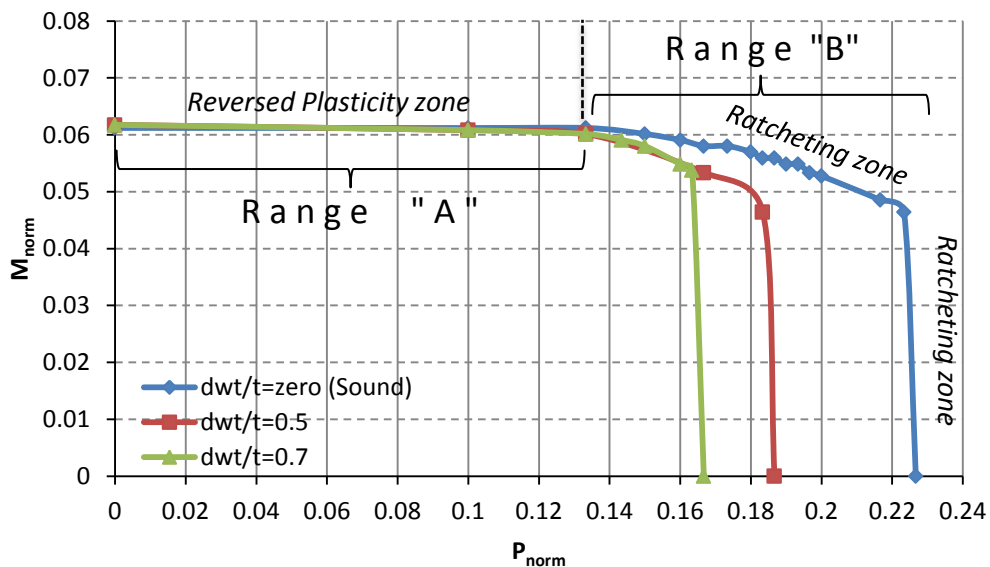


Figure 30: In-plane shakedown limit boundary when the local wall thinning lies on the run-pipe

#### 4.2.1.1 Shakedown results when the local wall thinning lies on the run-pipe opposite to the branch-pipe

When local wall thinning lies on the run-pipe, shakedown moment boundary does not change, for any value of the local wall thinning depth, except for the inclined range (B) in in-plane bending situation, as shown in Figs. 30 and 31. On the other hand, according to the shakedown pressure, it decreases with the increase of the local wall thinning depth. The cause of this may be also the same of the limit load analysis as follows; when the local wall thinning lies on the run-pipe opposite to the intersection, it lies on the zero-reaction moment of the simply supported run pipe, as shown in Fig. 26. Therefore, when the moment and pressure are applied, it is not stressed by the moment, but the only load that has an effect on the local wall thinning area is the pressure load. This cause is applicable till the beginning of the ratcheting zone (range “B”) that has a combined effect of moment and pressure.

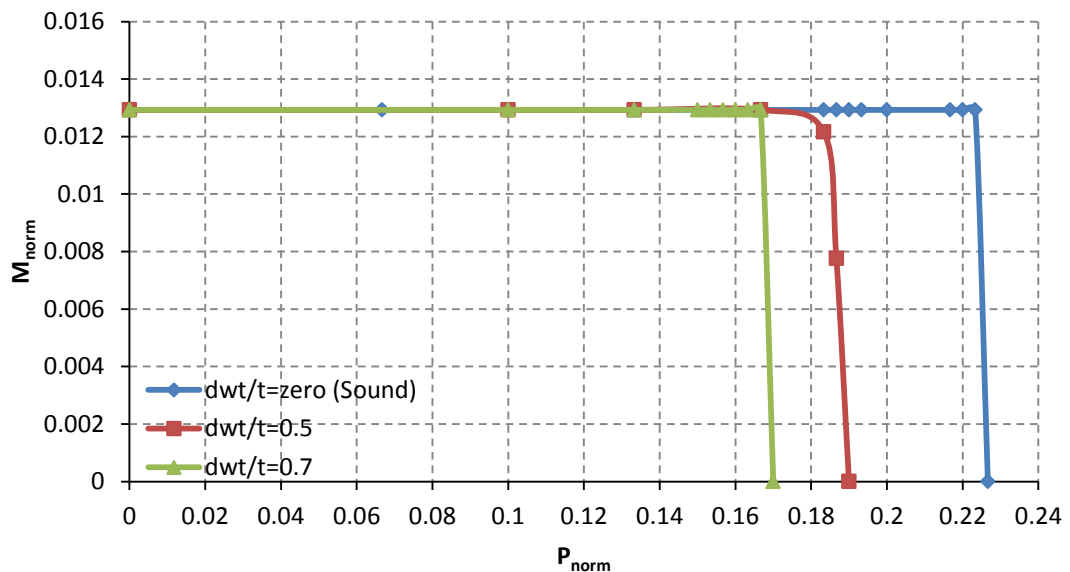


Figure 31: Out-of-plane shakedown limit boundary when local wall thinning lies on the run-pipe

4.2.1.2. *Shakedown results when the local wall thinning lies on the branch-pipe next to the intersection*

For the local wall thinning lies on the branch next to the intersection, the shakedown moment and pressure boundaries decrease with the increase of the local wall thinning depth in both plateau and inclined ranges. Unlike the situation of local wall thinning lies on the run-pipe, the local wall thinning lies on the maximum reaction bending moment in the simply supported run-pipe bending moment diagram in Fig. 26. Therefore, the effect of local wall thinning appears in both pressure and bending moment limits, as shown in Figs. 32 and 33.

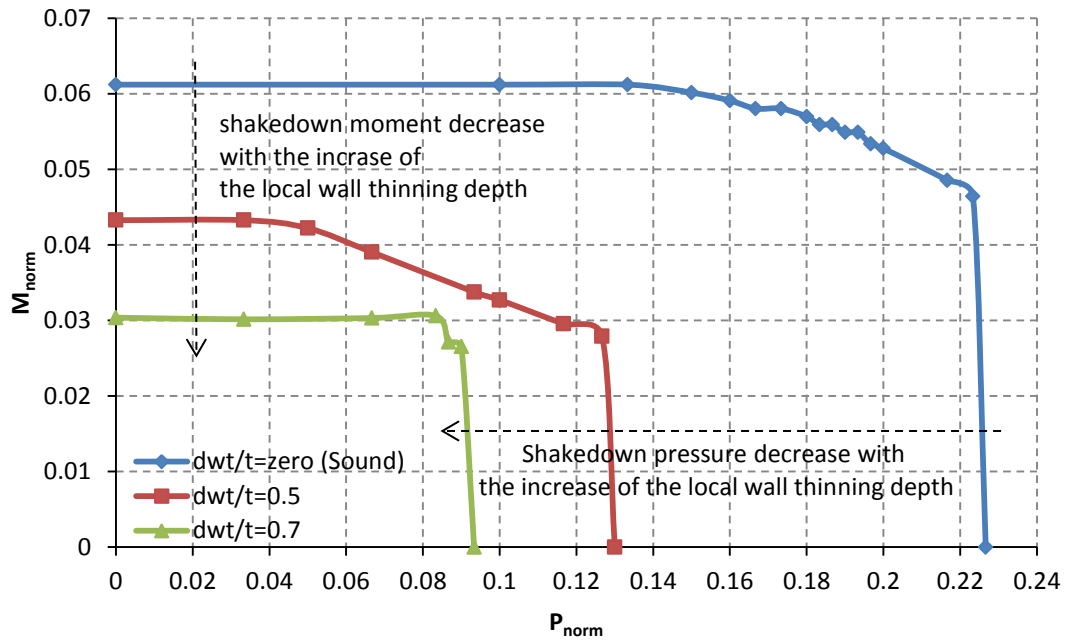
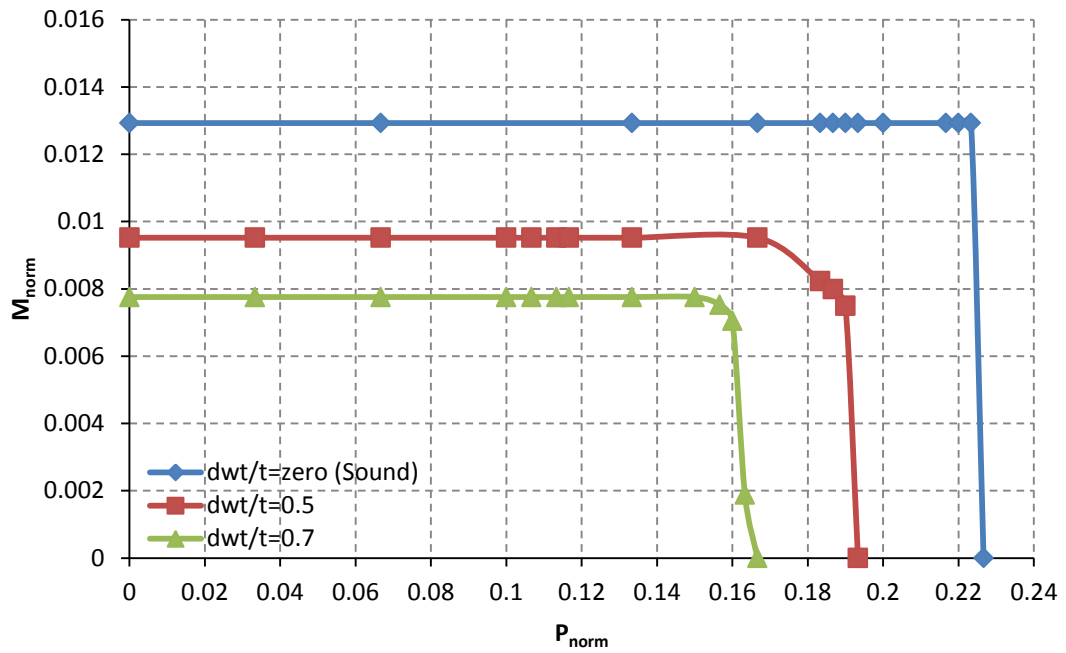


Figure 32: In-plane shakedown moment limit boundary when the local wall thinning lies on the branch



**Figure 33: Out-of-plane shakedown moment limit boundary when the local wall thinning lies on the branch**

When bending moment was applied in the out-of-plane direction with the run-pipe axis, the bending moment has a plateau all over the pressure range, except for negligible pressure range. This is when the local wall thinning lies on the run-pipe or on the branch, as shown in Figs. 31 and 33. This means that this situation has only a reversed plasticity failure behavior except when exceeding the  $P_{SD}$  limit it has a ratcheting failure behavior.

Generally, in the limit load and shakedown limit analyses, the limit moment values, when the moment is applied on the branch in the in-plane direction, has more than double the value of the limit moment when it is applied on the branch in the out-of-plane direction, as shown in all previous limit and shakedown boundary curves.

#### 4.2.2. The effect of the local wall thinning depth on the shakedown limit load

For further analysis of the shakedown results, a shakedown limit moment analysis was conducted for four different local wall thinning depths  $0 \leq d_{wt}/t \leq 0.7$  while no pressure was applied (zero-value steady pressure). The only location of the local wall thinning was considered is when it lies on the branch, as if it lies on the run-pipe, local wall thinning has no effect on the shakedown limit moment. The shakedown limit moment was plotted to show a linear decrease of the shakedown limit moment against these ratios, as shown in Fig. 34.

As the shakedown limit moment is constant through the reversed plasticity pressure range (A), the shakedown moment loads versus  $d_{wt}/t$  ratio graphs are applicable only for this pressure range. The inclined range (B) does not have a uniform relation with the local wall thinning depth as noticed in the previous boundary curves.

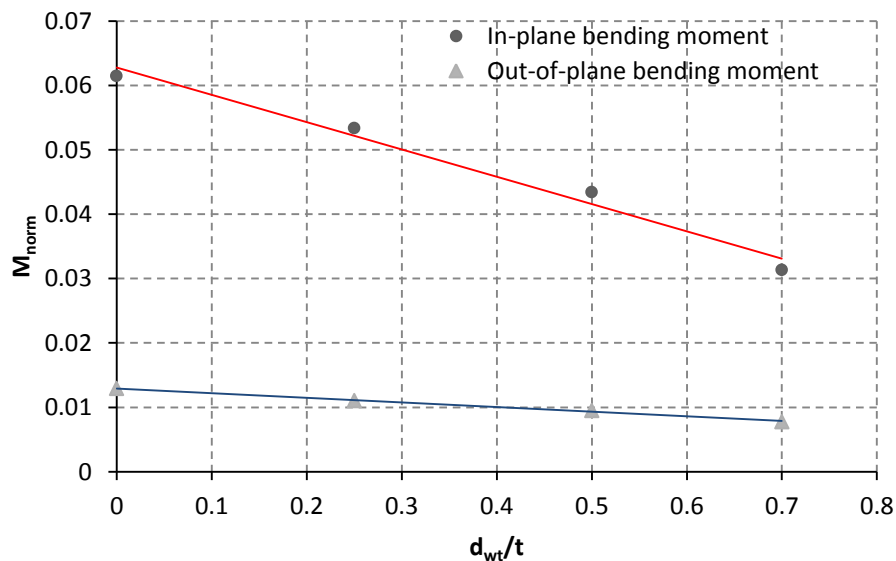
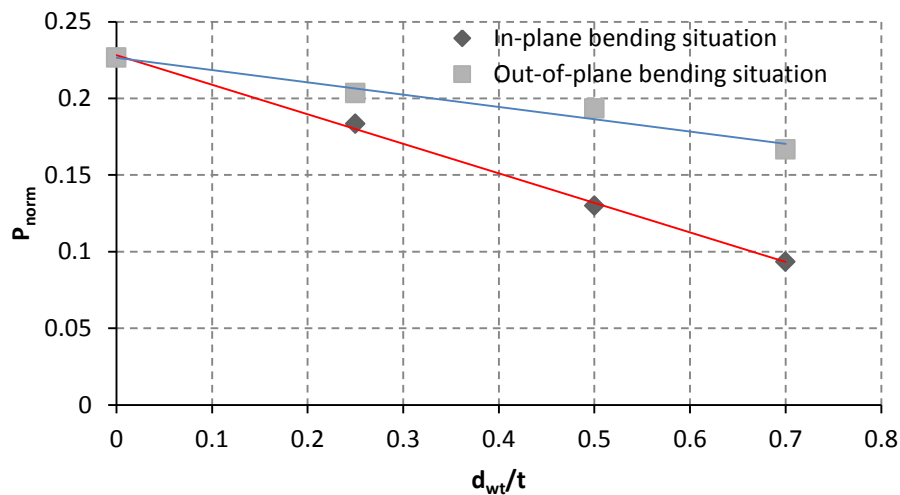


Figure 34: The effect of the local wall thinning depth on the in-plane and out-of-plane shakedown bending moments, when it lies on the branch

When local wall thinning lies at the maximum tension side of in-plane and out-of-plane bending, the shakedown pressure ( $P_{SD}$ ) was determined for the same values of local wall thinning depths. The shakedown pressure was plot against the local wall thinning depth to show also a linear decrease. The in-plane situation experiences also a higher drop than the out-of-plane one, as shown in Fig. 35.



**Figure 35: The effect of the local wall thinning depth on the shakedown pressure, when it lies on the branch at max tension side of in-plane and out-of-plane situations**

As noted in API 579 standard that the minimum measured thickness ( $t_{mm}$ ) cannot reach 0.2 of the nominal thickness, as this is a limit to retire the component for the criteria of level 1 and 2 assessments. When the local wall thinning exceeds the 0.8  $d_{wt}/t$  ratio, the shakedown limit load and limit load experience high nonlinearities of stresses (high stress concentration) because of the high drop of the thickness. Therefore, this may the same reason of the sudden drop of the shakedown pressure and moment when the thinning exceeds 0.7  $d_{wt}/t$  ratio. Therefore, the curves were plotted till 0.7  $d_{wt}/t$  ratio only, as it is valid up to this limit.

## **CHAPTER 5: SHAKEDOWN RESULTS VERIFICATION USING API 579 STANDARD, LEVEL-THREE ASSESSMENT PROCEDURES**

The illustrated results and discussion of the shakedown limit moment boundary and the effect of the local wall thinning on these limits were achieved for serving the main objective of this research. Now, it will be verified and compared with results of the existing shakedown assessment procedures in API 579 standard. Therefore, these comparisons are to validate the proposed assessment procedure that is based on the Simplified Technique to be used for locally thinned wall components.

### **5.1. *Shakedown limit assessment (elastic stress analysis)***

As illustrated in section 2.5.2 that API 579 standard used the elastic shakedown limit analysis as a linear approximation for determination of the shakedown limit loads. The condition used in the elastic analysis for shakedown limit determination is when the elastic von Mises stress field hypothetically reaches a double of the yield strength of the material, with the assumption of elastic-perfectly-plastic material model.

This elastic analysis was conducted for five different selected samples of the shakedown results of the Simplified Technique. The samples were selected from the local wall thinning lies on the branch results to compare the two techniques using different cases of the local wall thinning depths, moment directions, and pressures, as shown in Table 5.

**Table 5: Comparison of the Simplified Technique results with API 579, Shakedown limit assessment using elastic stress analysis**

#	$d_{wt}/t$	Location of Local wall thinning	Moment direction	Pressure ( $P_{norm}$ )	Shakedown moment using the Simplified Technique (MPa)	Shakedown moment using Elastic analysis API (MPa)	Discrepancy (%)
1	Sound	on branch	In-plane	5.5	289,843	215,000	25.82
2	Sound	on branch	In-plane	1.5	317,187	305,000	3.84
3	0.5	on branch	In-plane	1.5	202,343	195,000	3.63
4	Sound	on branch	Out-of-plane	4	137,500	110,000	20
5	0.5	on branch	Out-of-plane	4	101,250	85,000	16.05

From the comparison, results of the elastic analysis have a varying discrepancy when it is compared to the Simplified Technique, but the elastic analysis is always more conservative. This is because the elastic analysis is based on a uniaxial stress field, like in tension tests, but the considered pipe-branch connection (the validation case study) has a multi-axial stress field and quite complex geometry that lead to several stress concentration areas. Overall, the existing elastic analysis has the advantage of the simplicity of the numerical analysis, as it is a linear method and it has no elastic-plastic analysis. On the other hand, it has a wide varying conservative discrepancy than any elastic-plastic analysis.

## 5.2. *Shakedown limit assessment (elastic-plastic stress analysis)*

As illustrated in section 2.5.1, API 579 standard applies a full cyclic elastic-plastic analysis for shakedown limit load determination of multi-axial stress field, like pipe-branch connection case. It directly applies the time history of the loading and unloading of the component. Therefore, all cases of the shakedown results from the Simplified Technique were verified using this analysis and it agreed with the results for the same numerical number of increments of both numerical analyses.



All limit moment boundary curve points were verified using this analysis, including all the break points between ratcheting and reversed plasticity regions, all points of  $P_{SD}$  pressure value, and all points from the reversed plasticity and ratcheting regions to verify every detail of the shakedown limit curve. A case was selected for illustration has a normalized pressure of 0.03, in-plane bending moment, and a local wall thinning lies on the branch-pipe next to the intersection with 0.5  $d_{wt}/t$  ratio. From shakedown moment boundary curve in Fig. 32, the normalized shakedown moment was determined to be 0.043 using the Simplified Technique. When the moment was increased to 0.046 and full cyclic loading elastic-plastic analysis was performed, reversed plasticity behavior was observed, as shown in von Mises equivalent stress versus plastic equivalent strain graph in Fig. 36. The sign of the mean stress was taken beside the von Mises equivalent stress to show if the yield is in tension or in compression. Therefore, the behavior can be determined if it is ratcheting or reversed plasticity, through the progress of the plastic strain, as shown in Figs. 36 and 37.

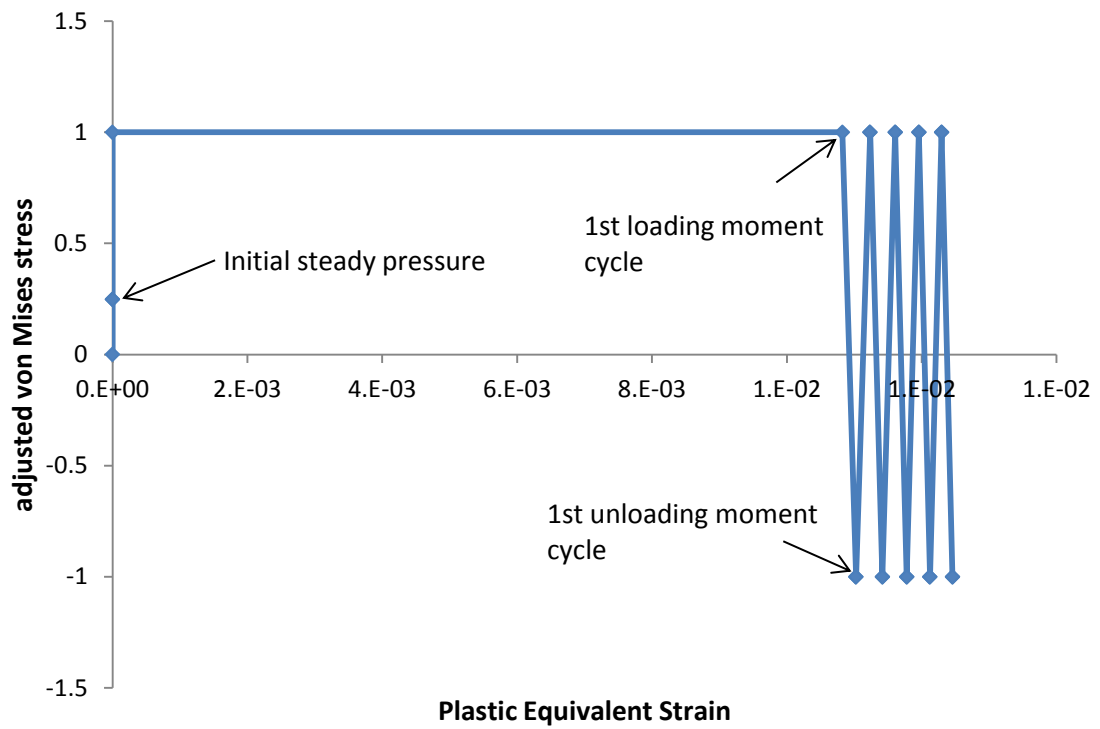


**Figure 36:Equivalent stress VS. equivalent plastic strain curve of reversed plasticity behavior**

Also the same analysis was conducted for the same conditions but with a normalized pressure of 0.1 that resulted a normalized shakedown moment of 0.033. When the bending moment was increased to reach 0.036, the ratcheting behavior was observed when plotting the von Mises equivalent stress versus equivalent plastic strain, as shown in Fig. 37. By comparing the results of the Simplified Technique assessment procedure and the elastic-plastic analysis assessment procedure, they agreed for all values of shakedown limit boundary points.

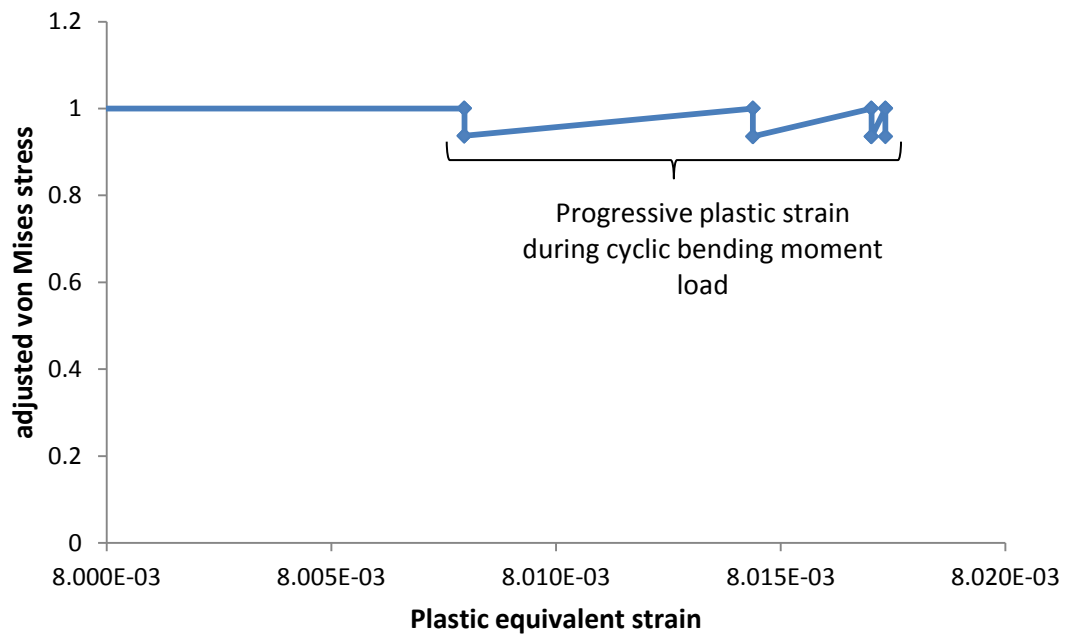


**Figure 37: Von Mises stress VS. equivalent plastic strain curve of ratcheting behavior**

## CHAPTER 6: CONCLUSION

### 6.1. *The limit load analysis*

A limit load analysis was conducted to the FE model of the previously selected locally thinned wall pipe-branch connection utilizing the Twice-Elastic Slope method. Bending moment loading was applied on the branch with the existence of a steady internal pressure spectrum. Limit moment boundary curves were generated and the following conclusions were noticed:

- When local wall thinning lied on the branch next to the intersection, the combined limit bending moment and internal pressure decreased with the increase of the local wall thinning depth. The generated limit moment boundary curves illustrated the same elliptical curvature of Tabone and Mallette [13] and Xuan et al. [11], but with lower limit load of the corresponding single load situations ( $P_{SL}$  and  $M_{SL}$ ).
- When local wall thinning lied on the run-pipe opposite to the branch, failure always happens at the maximum tension side on the intersection line due to the bending moment, not in the locally thinned wall area. Therefore, the local wall thinning depth has no effect on the limit moment as long as the pressure is not sufficient to cause failure alone in locally thinned wall area on the run-pipe.
- For the location of local wall thinning, it is more critical (depending upon the pressure capacity) to lie on the branch at maximum tension side of in-plane bending moment than to lie on the maximum tension side of out-of-plane bending or on the run-pipe cases.

- The area replacement method in API 579 standard showed conservative results compared to the results of the numerical limit pressure analysis. Meanwhile, it did not show decrease of pressure limit with the increase of the local wall thinning depth as the numerical limit pressure analysis outcomes revealed.
- The limit analysis method in API 579 standard showed a linear decrease in pressure limit with the increase of local wall thinning depth. The minimum magnitude of the pressure limit approximately equals to the area replacement method constant value. Hence, the limit analysis method provides less conservative results than the area replacement method and close results to the numerical limit analysis which showed a quadratic decrease pattern of the pressure limit.

## 6.2. *The shakedown analysis*

A shakedown limit load analysis was conducted concerning the FE model of the previously selected locally thinned wall pipe-branch connection. Cyclic bending moment was applied on the branch with the existence of a steady internal pressure spectrum. The newly proposed shakedown assessment procedure was utilized to generate the shakedown limit moment boundary curves revealing the following conclusions:

- When local wall thinning lied on the run-pipe opposite to the branch, the shakedown bending moment applied on the branch was not affected by the local wall thinning depth; however, the shakedown pressure ( $P_{SD}$ ) decreased.
- When local wall thinning lied on the branch next to the intersection at the maximum tension side of the bending moment (when an out-of-plane bending

moment was applied on the branch) the failure always occurred due to reversed plasticity till the steady internal pressure exceeded the shakedown pressure ( $P_{SD}$ ). On the other hand, when an in-plane bending moment was applied on the branch, failure occurred due to reversed plasticity or ratcheting depending on the internal pressure loading for the currently analyzed geometry.

- For the location of local wall thinning, it is more critical to be on the branch at maximum tension side of in-plane bending moment than to be at the maximum tension side of out-of-plane bending or on the run-pipe. This conclusion depends upon the internal pressure magnitude, and the slope of the linear decrease of the bending moment magnitude against local wall thinning depth.
- When the proposed shakedown assessment procedure outcomes were compared to the outcomes of the linear elastic analysis of API 579 standard, the latter analysis or methodology showed extreme conservatism in all cases.
- When the proposed shakedown assessment procedure outcomes were checked using full elastic-plastic cyclic loading analysis of API 579 standard, all results were in very good agreement with the proposed shakedown assessment procedure.

Finally, the proposed shakedown assessment procedure which is based on the Simplified Technique can be utilized for locally thinned wall components to determine the shakedown limit load. Therefore, the shakedown limit load can be obtained without performing lengthy time consuming full elastic-plastic cyclic loading FE analyses with acceptable accuracy for local wall thinning depth range (0 - 0.7 of the total thickness) and at any location within the structure.

## References

- [1] Hany F. Abdalla, Mohammad M. Megahed, and Maher Y.A. Younan, "A simplified technique for shakedown limit load determination," *Nuclear Engineering and Design*, pp. 1231-1240, 2007.
- [2] ASME and API, *API 579-1/ASME FFS-1.*, June 5, 2007.
- [3] Masato Ono, Ki Woo Nam, Koji Takahashi, and Kotoji Ando, "Effect of local wall thinning on fracture behavior of straight pipe," *ECF*, 2007.
- [4] Jin Weon Kim, Ho Lee Song, and Chi Yong Park, "Experimental evaluation of the effect of local wall thinning on failure pressure of elbows," *Nuclear engineering and Design*, vol. 239, no. 39, pp. 2737-2746, December 2009.
- [5] Hu Hui and Peining Li, "Plastic limit load analysis for steam generator tubes with local wall thinning," *Nuclear Engineering and Design*, pp. 2512-2520, 2010.
- [6] F-Z Xuan, P-N Li, and S-T Tu, "Evaluation of plastic limit load of piping branch junctions subjected to out-of-plane moment loadings," *J. Strain Analysis*, pp. 395-404, 2003.
- [7] J. Schroeder, "Experimental limit couples for branch moment loads on 4 in. ANSI B16.9 Tees," New York, N.Y., 1985.
- [8] N.C. Lind, A.N. Sherbourne, F.E. Ellyin, and J. Dainora, "Plastic tests of two

branch pipe connections," Wendt, 1971.

- [9] Yun-Jae Kim, Kuk-Hee Lee, and Chi-Yong Park, "Limit loads for piping branch junctions under internal pressure and in-plane bending - extended solutions," *International Journal of pressure vessels and piping*, pp. 360-367, 2008.
- [10] K.S. Lee, D.N. Moreton, and D.G. Moffat, "An approximate method for determining the limit pressure of piping branch junctions with  $d/D \leq 0.5$ ," in *ASME pressure vessels and piping conference*, San Antonio, 2008, pp. 273-280.
- [11] F. Z Xuan and P. N. Li, "Finite Element-based limit load of piping branch junctions under combined loadings," *Nuclear Engineering and Design*, vol. 231, pp. 141-150, 2004.
- [12] Fu-Zhen Xuan, Pei-Ning Li, and Chen Wang, "Experimental limit load of forged piping branch junction and comparison with existing solution," *Key Engineering materials*, pp. 1208-1213, 2005.
- [13] C. J. Tabone and Mallette R. H., "Pressure-plus-moment limit load analysis for a cylindrical shell nozzle," *ASME J. Pressure vessel Technology*, vol. 109, no. 1, pp. 297-301, 1987.
- [14] K-H Lee, Y-J Ryu, and C-Y Park, "Effect of local wall thinning on limit loads for piping branch junctions. Part 1: Internal pressure," *IMechE*, pp. 569-580, 2008.



- [15] K-H Lee, K-M Ryu, Y-J Kim, and C-Y Park, "Effect of local wall thinning on limit loads for piping branch junctions part2: in-plane bending," *The journal of strain analysis for engineering design*, pp. 581-594, 2008.
- [16] Y. J. Kim, D. J. Shim, K. Nikbin, S. S. Hwang, and J. S. Kim, "Finite element based plastic limit loads for pipes with part through surface cracks under combined loading," *International Journal for pressure vessels and piping*, pp. 527-540, 2003.
- [17] "ASME B31," 2010.
- [18] Melan, "Der Spannungszustand eins Mises-Henckyschen Kontinuums bei veraederlicher Belastung," *Sitzber. Akad. Wiss.*, pp. 73-78, 1938.
- [19] R. Seshadri, "The generalized local strain (GLOSS) analysis-theory and applications," *Journal of pressure vessel technology*, pp. 219-227, 1991.
- [20] L. Qian and Z. Wang, "Structural limit and shakedown analysis: A thermo-parameters method," in *ASME pressure vessels and piping conference*, 1990, pp. 47-53.
- [21] Donald Mackenzie and James T. Boyle, "A simple method for estimating shakedown load for complex structure," *Journal of pressure vessel technology*, pp. 89-94, 1993.

- [22] A. R. S. Ponter and K. F. Carter, "Shakedown state simulation technique based on linear elastic solutions," *Comput Meth Appl Mech Engng*, pp. 259-279, 1997.
- [23] Hany F. Abdalla, Mohammad M. Megahed, and Maher Y.A. Younan, "Determination of shakedown limit load for a 90-degree pipe bend using a simplified technique," *Journal of pressure vessel technology*, 2007.
- [24] Hany F. Abdalla, M. Y. Younan, and M. M. Megahed, "Determination of shakedown limit loads for a cylindrical vessel-nozzle intersection via a simplified technique," *Pressure Vessels and Piping*, 2011.
- [25] C. Nadarajah, D. Mackenzie, and J. T. Boyle, "Limit load and shakedown analysis of nozzle/cylinder intersection under internal pressure and in-plane moment loading," *International Journal of Pressure Vessels and Piping*, 86, pp. 261-272, 1996.
- [26] W. A. Macfarlane and G.E. Findlay, "A simple technique for calculating shakedown loads in pressure vessels," *IMechE*, 186, pp. 4-72, 1978.
- [27] M. Robinson, "Lower bound limit pressure for the cylinder-cylinder intersection - A parametric survey," *Journal of pressure vessel technology*, pp. 65-73, 1978.
- [28] Hany Abdalla, Mohamed Megahed, and Maher Younan, *A Simplified Technique for shakedown limit load determination with application to 90-degree pipe bends.*: Cairo University, 2009.

- [29] Fu-Zhen Xuan, Pei-Ning Li, and Shan-Tung Tu, "Limit load analysis for the piping branch junctions under in-plane moment," *International Journal of Mechanical Sciences*, pp. 460-467, 2006.
- [30] B.H. Wu, Z.F. Sang, and G. E. O. Widera, "Plastic analysis of cylindrical vessels under in-plane moment on the nozzle," *Journal of pressure vessel technology*, 132, pp. PP. 061203-1 -061203-8, 2010.
- [31] K-M Ryu, K-H Lee, Y-J Kim, and C-Y Park, "Effect of local wall thinning on limit loads for piping branch junctions part1: Internal pressure," *The Journal of strain analysis for engineering design*, pp. 569-580, 2008.
- [32] D.L. Marriott, "Evaluation of deformation or load control of stress under inelastic conditions using finite elements stress analysis," *ASME PVP trans.*, pp. 3-9, 1988.
- [33] Yun-Jae Kim, Kuk-Hee Lee, and Chi-Yong Park, "Limit loads for thin-walled piping branch junctions under internal pressure and in plane bending," *International Journal of Pressure Vessels and Pipings*, pp. 645-653, 2006.
- [34] M. R. Jones and J. M. Eshelby, "Limit solutions for circumferential cracked cylinders under internal pressure and combined tension and bending," UK, 1990.
- [35] Y. A. Hafiz, M. Y. Younan, and H. F. Abdalla, "Limit and Shakedown loads determination for locally thinned wall pipe branch connection subjected to

pressure and bending moments," in *ASME Pressure Vessels and Piping Conference*, Toronto, Canada, 2012.